



Computing Complex Flows using a Front Tracking Method

Grétar Tryggvason
Worcester Polytechnic Institute

*Workshop on Numerical methods for the solution of
PDEs on non-body fitted grids
MARATEA (Italy)
May 13-15, 2010*



DNS of Multiphase Flows Outline

Motivation

Numerical approach

Simulations of bubbly channel flows

More complex systems

- Other fields

- Boiling

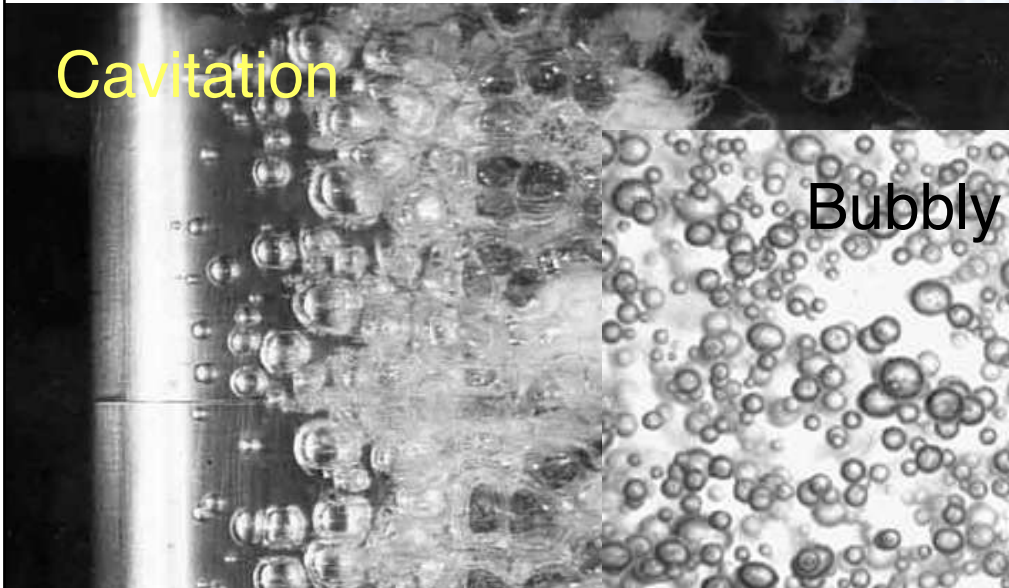
- Multiscale issues

Outlook and current issues

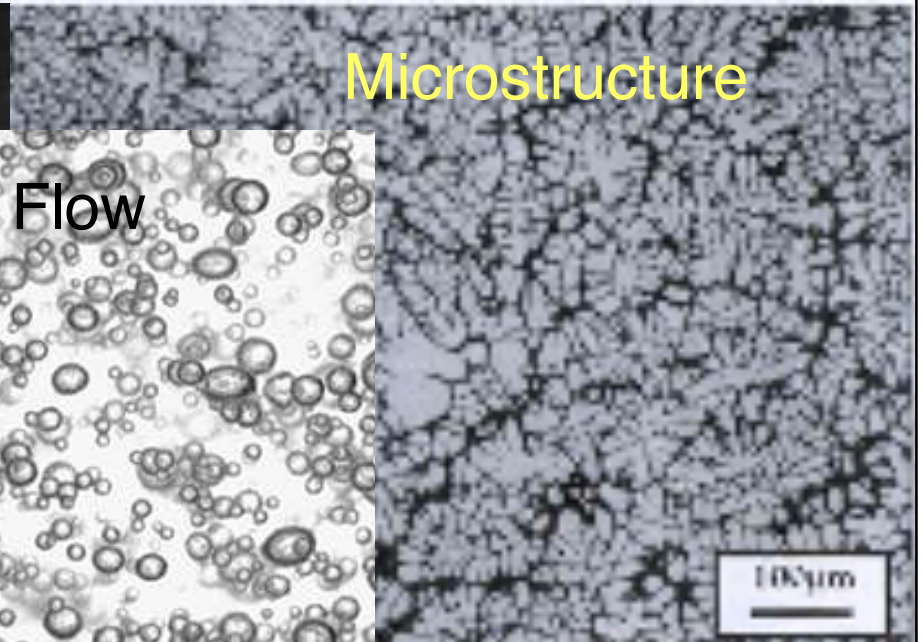
DNS of Multiphase Flows

Motivation and Goals

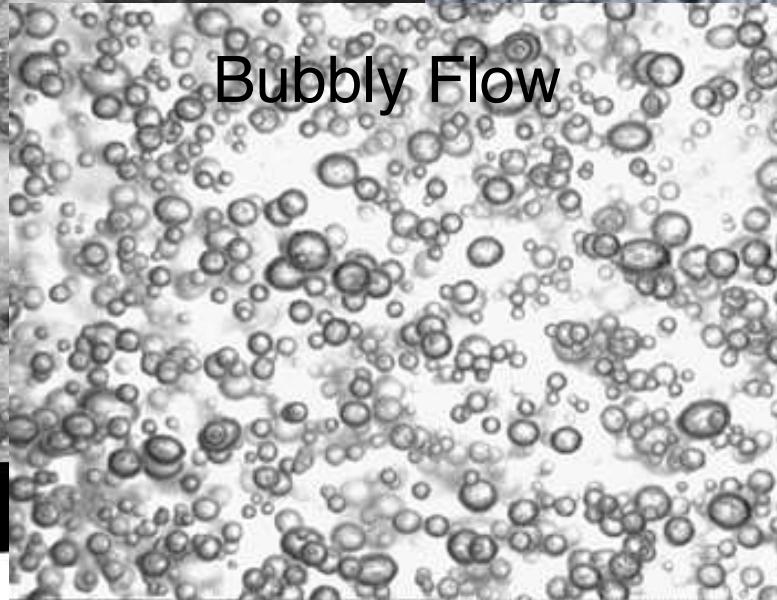
Cavitation



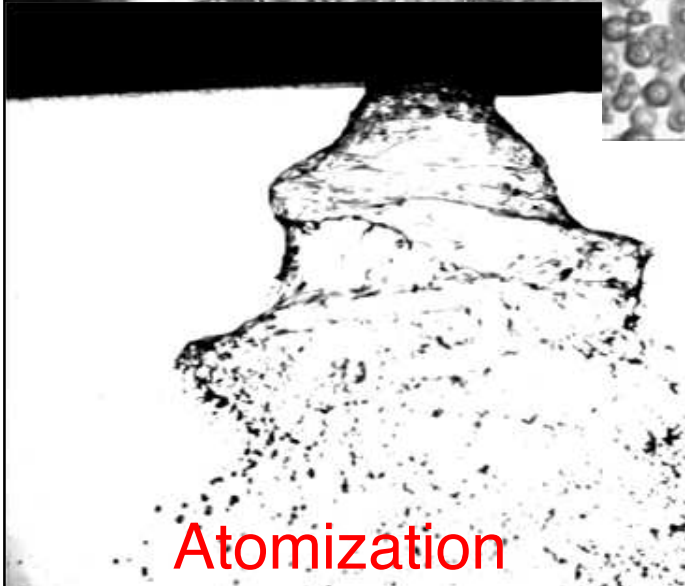
Microstructure



Bubbly Flow



Atomization



Splash



School of fish





DNS of Multiphase Flows

Motivation and Goals

The goal is to simulate accurately the smallest continuum scales for multiphase systems that are sufficiently large so that meaningful averages can be obtained and the results used to help generate insight and closure models for engineering tools

Example: The “two-fluid model”

$$\frac{\partial}{\partial t} \epsilon_p \rho_p + \nabla \cdot (\epsilon_p \rho_p \mathbf{u}_p) = \dot{m}_p$$

$$\frac{\partial}{\partial t} (\epsilon_p \rho_p \mathbf{u}_p) + \nabla \cdot (\epsilon_p \rho_p \mathbf{u}_p \mathbf{u}_p) = -\epsilon_p \nabla p_p$$

$$+ \nabla \cdot (\epsilon_p \mu_p \mathbf{D}_p) + \epsilon_p \rho_p \mathbf{g} + \nabla \cdot (\epsilon_p \rho_p \langle uu \rangle) + \mathbf{F}_{\text{int}}$$

Equations for the average motion of each constituent

Reynolds stresses interfacial forces

Volume average of f_i

$$\langle f_i \rangle = \frac{1}{\epsilon_i \text{Vol}} \int_V \chi_i(\mathbf{x}, t) f_i(\mathbf{x}, t) dv$$

Characterization of the interface

$$\frac{1}{\text{Vol}} \int_s \mathbf{n} \mathbf{n} da \quad \frac{1}{\text{Vol}} \int_s \mathbf{n} \mathbf{n} \mathbf{n} \mathbf{n} da$$

Structure functions, turbulent quantities, etc.



Computational Approach



DNS of Multiphase Flows Numerical Method

CFD of Multiphase Flows—one slide history

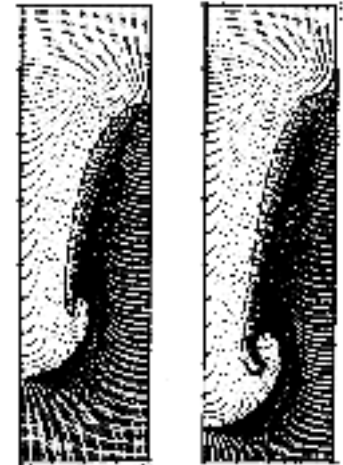
BC: Birkhoff and boundary integral methods for the Rayleigh-Taylor Instability

65' Harlow and colleagues at Los Alamos:
The MAC method

75' Boundary integral methods for Stokes flow and potential flow

85' Alternative approaches (body fitted, unstructured, etc.)

95' Beginning of DNS of multiphase flow. Return of the “one-fluid” approach and development of other techniques



From: B. Daly (1969)

Conservation of Momentum

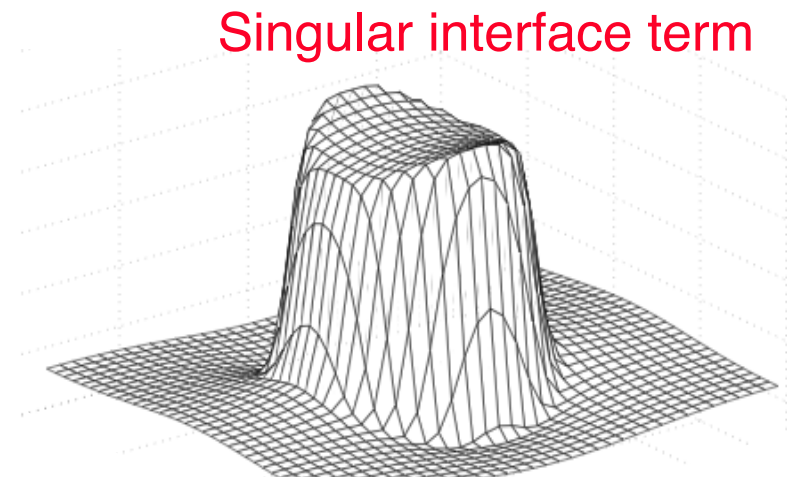
$$\rho \frac{\partial \mathbf{u}}{\partial t} + \rho \nabla \cdot \mathbf{u} \mathbf{u} = -\nabla p + \mathbf{f} + \nabla \cdot \mu (\nabla \mathbf{u} + \nabla^T \mathbf{u}) + \int_F \sigma \kappa \mathbf{n} \delta(\mathbf{x} - \mathbf{x}_f) da$$

Conservation of Mass

$$\nabla \cdot \mathbf{u} = 0 \quad \text{Incompressible flow}$$

Equation of State:

$$\frac{D\rho}{Dt} = 0; \quad \frac{D\mu}{Dt} = 0 \quad \text{Constant properties}$$



Oscillating drop: pressure

The conservation equations are solved on a regular fixed grid and the front is tracked by connected marker points.

The “one fluid” formulation of the conservation equations is the starting point for several numerical methods, including MAC, VOF, level sets, and front tracking.

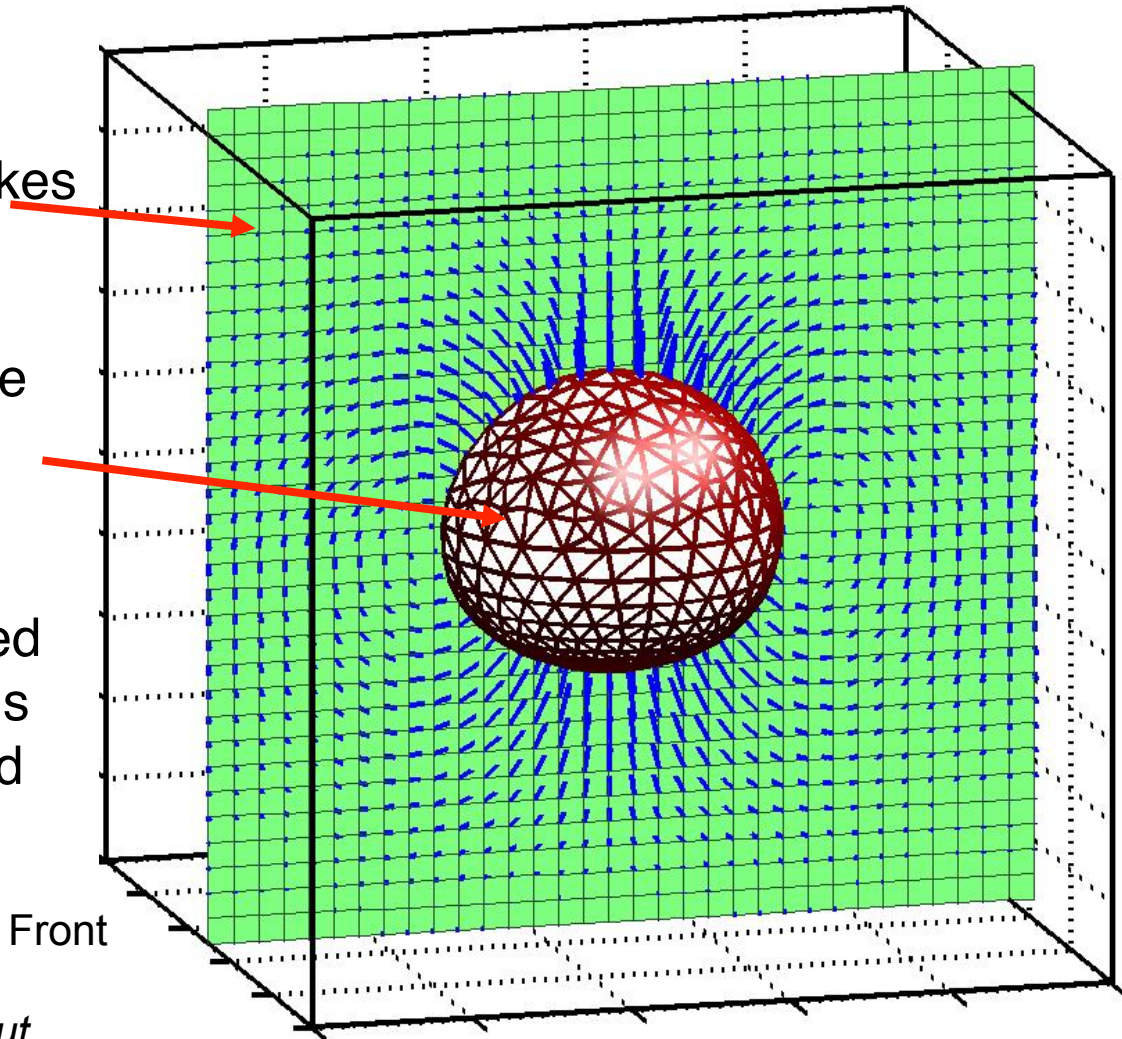
Front Tracking

Fixed grid used for the solution of the Navier-Stokes equations

Tracked front to advect the fluid interface and find surface tension

The method has been used to simulate many problems and extensively tested and validated

S.O. Unverdi, G. Tryggvason. "A Front Tracking Method for Viscous Incompressible Flows." *J. Comput. Phys*, 100 (1992), 25-37.



The velocities are interpolated from the grid:

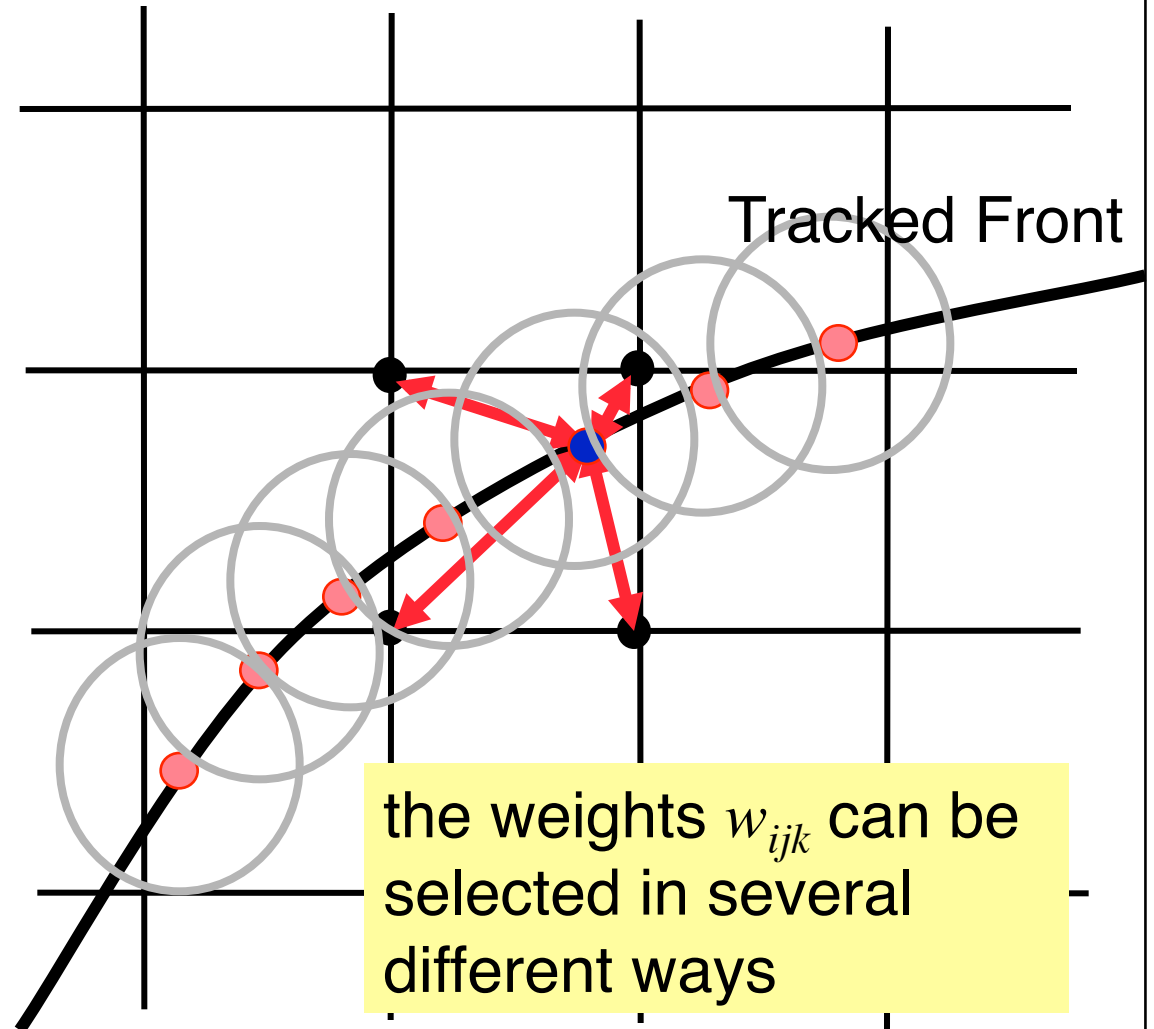
$$\phi_l = \sum \phi_{ijk} w_{ijk}$$

The front values are distributed onto the grid by

$$\phi_{ijk} = \sum \phi_l w_{ijk} \frac{\Delta s_l}{h^3}$$

On the front: per length
On the grid: per volume

Finite Difference Grid



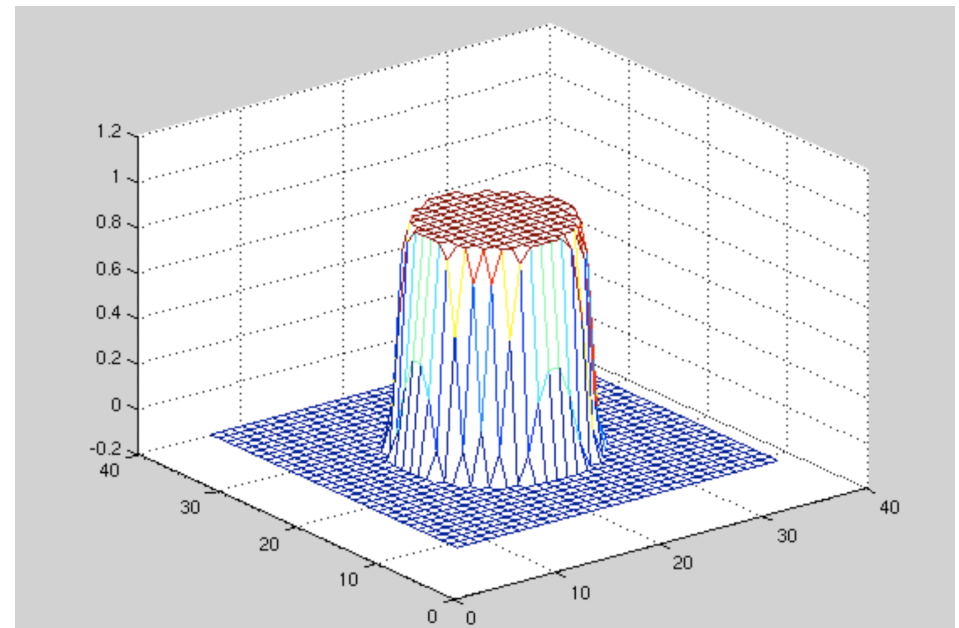
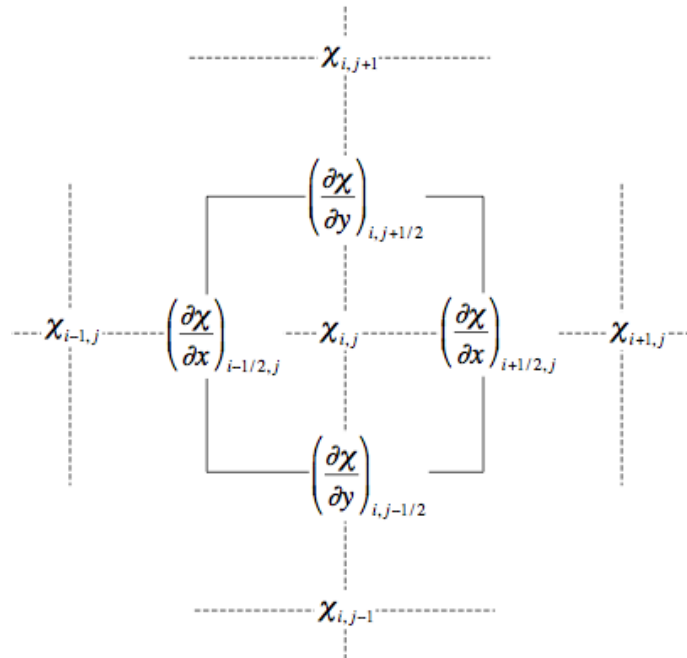
Construction of the density from the gradient

$$\chi_{i,j} = \chi_{i-1,j} + \Delta x \left(\frac{\partial \chi}{\partial x} \right)_{i+1/2,j}$$

$$\chi_{i,j} = \frac{1}{4} \left(\chi_{i+1,j} + \chi_{i-1,j} + \chi_{i,j-1} + \chi_{i,j+1} + \right.$$

$$\left. \Delta x \left(\frac{\partial \chi}{\partial x} \right)_{i+1/2,j} - \Delta x \left(\frac{\partial \chi}{\partial x} \right)_{i-1/2,j} + \Delta y \left(\frac{\partial \chi}{\partial y} \right)_{i,j+1/2} - \Delta y \left(\frac{\partial \chi}{\partial y} \right)_{i,j-1/2} \right)$$

Solved in a narrow band around the interface

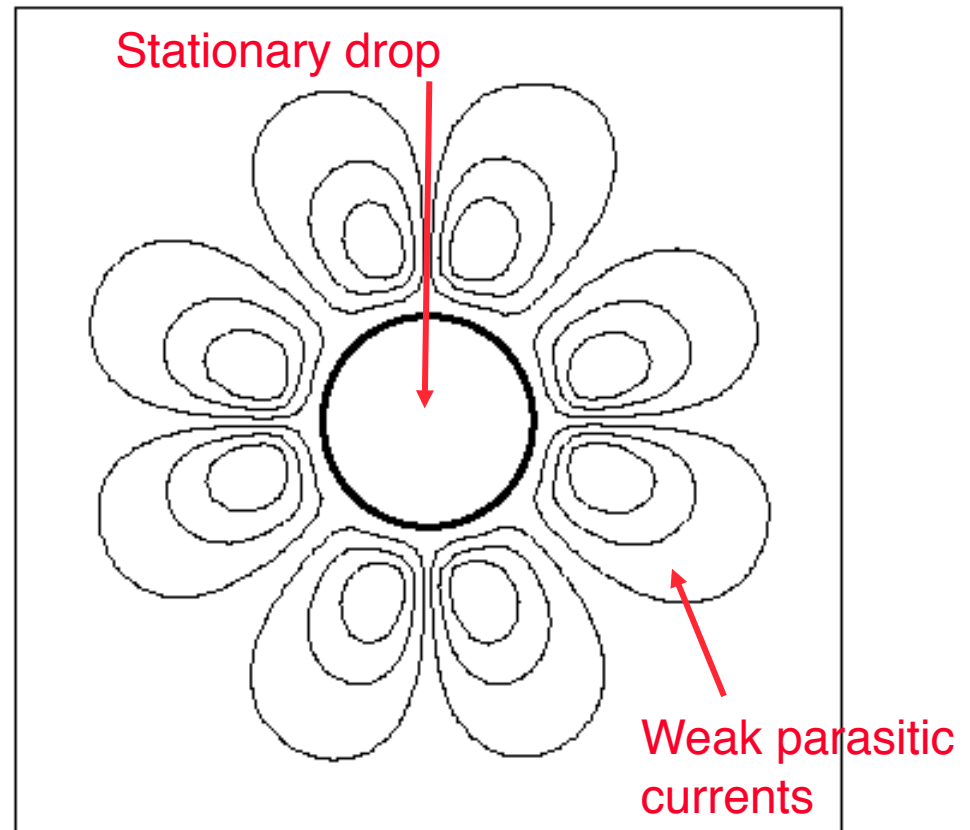


Parasitic Currents

The regular grid induces a small anisotropy. These currents are typically small in immersed boundary methods.

At steady state the pressure gradient should be balanced by surface tension

$$\nabla_h p + \mathbf{f}_\sigma^n = 0$$





DNS of Multiphase Flows

Numerical Method—Surface Tension

Surface tension can be added in several ways:

$$\mathbf{f}_{ij} = (\sigma\kappa)_{ij} \nabla I_{ij}$$

grid-grid

Curvature and normal vector computed directly on the fixed grid—marker function

$$\mathbf{f}_{ij} = (\sigma\kappa)_{ij}^f \nabla I_{ij}^f$$

front-front

Curvature and normal vector computed on the front, distributed to the fixed grid—our original approach

$$\mathbf{f}_{ij} = (\sigma\kappa)_{ij}^f \nabla I_{ij}$$

front-grid

Curvature computed on the front, distributed to the fixed grid. Normal vector computed on the grid

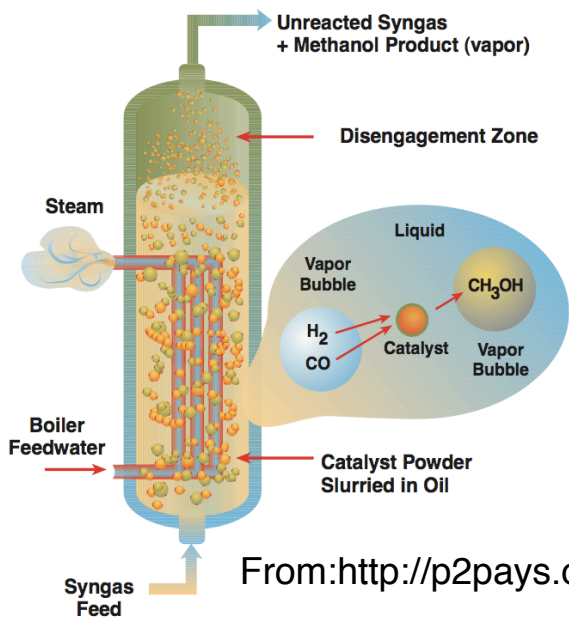
The last approach seems to combine the accuracy of tracking with the possibility of balancing pressure exactly



Bubbly Flows

DNS of Multiphase Flows

Why Multiphase Flows are Important!



Liquid Phase Methanol (LPMEOH™) Process

From: <http://p2pays.org/ref/16/15865.pdf>

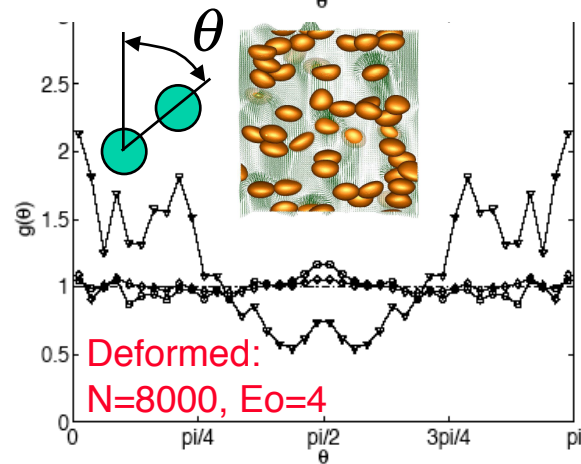
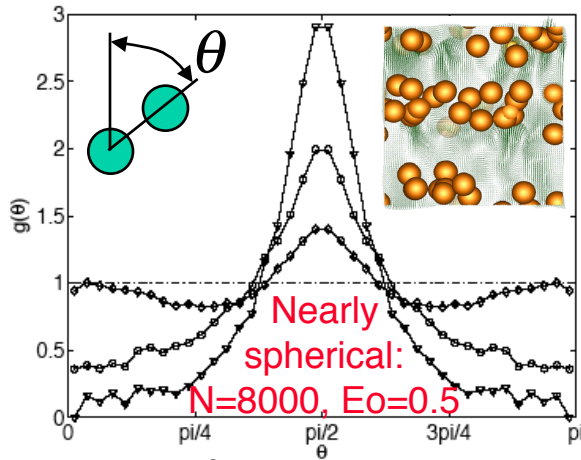


Examples of Applications of Bubble Columns

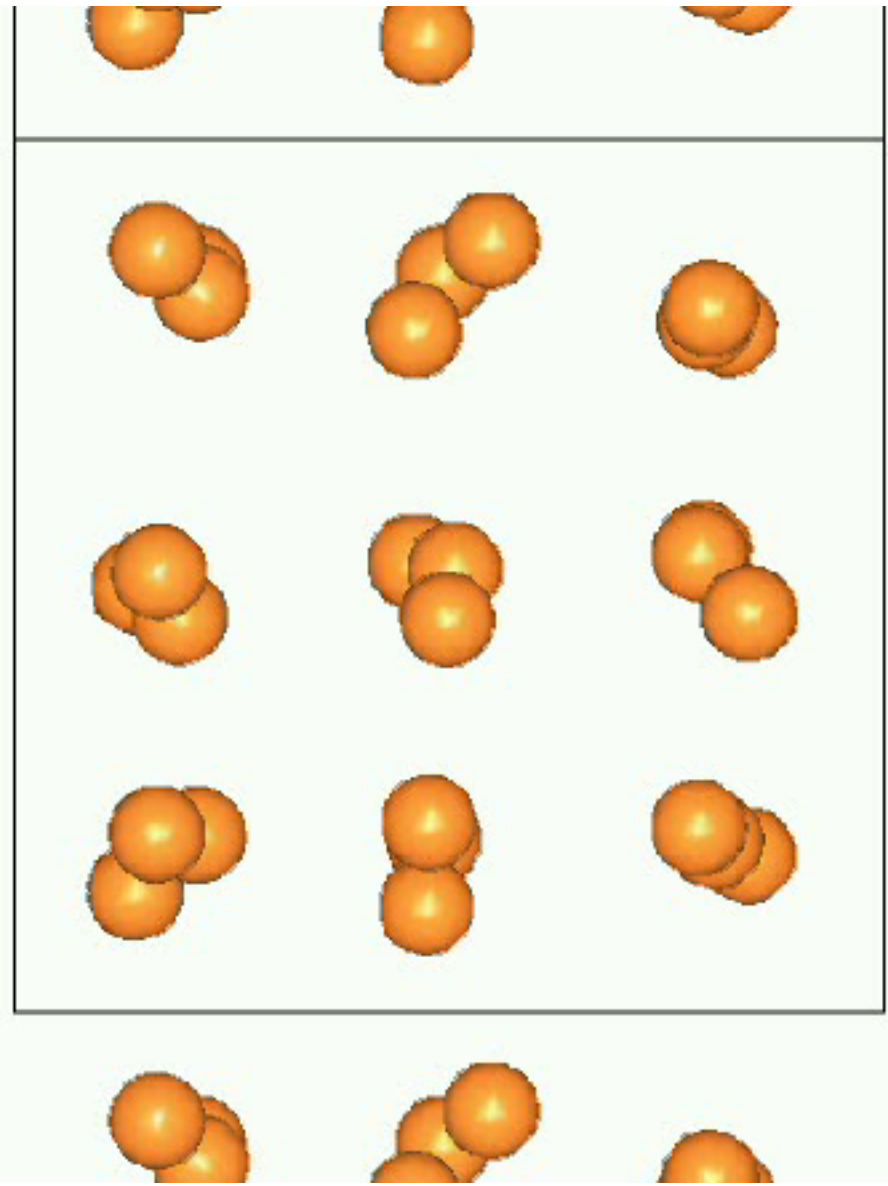
Process	Methods and/or Reactants
Acetone	Oxidation of cumene
Acetic acid	Oxidation of acetaldehyde
	Oxidation of sec-butanol
	Carbonylation of methanol
	Oxidation of acetaldehyde
Acetic anhydride	Partial oxidation of ethylene
Acetaldehyde	Oxidation of ethylbenzene
Acetophenone	Barium sulfide and chlorine
Barium chloride	Oxidation of toluene
Benzoic acid	Aqueous calcium oxide and chlorine
Bleaching powder	Aqueous sodium bromide and chlorine
Bromine	Absorption in aqueous solutions of sulfuric acid
Butene	Absorption in ammoniated brine
Carbon Dioxide	Carbon disulphide and chlorine
Carbone tetrachloride	Oxidation of cuprous chloride
Copper oxychloride	Oxidation of phenol
Cumene	Copper and cupric acid or hydrochloric acid
Cupric chloride	Oxychlorination of ethylene
Dichlorination	Benzene and ethylene
Ethyl benzene	Benzene and chlorine
Hexachlorobenzene	Oxidation of hydroquinone
Hydrogen peroxide	Absorption in aqueous solutions of sulfuric acid
Isobutylene	Oxidation of xylene
Phtalic acid	Oxidation of cumene
Phenol	Aqueous potassium carbonate
Potassium bicarbonate	Aqueous sodium carbonate
Sodium bicarbonate	Carbon dioxide, aqueous sodium carbonate, and sulfur dioxide
Sodium metabisulphides	Dithiocarbamates, chlorine, and air
Thiuram disulphides	Oxidation of ethylene in acetic acid solutions
Vinyl acetate	Wet oxidation of waste water
Water	

After: S. Furusaki, L.-S. Fan, J. Garside.
The Expanding World of Chemical Engineering (2nd ed), Taylor & Francis
2001

Angular pair probability distribution



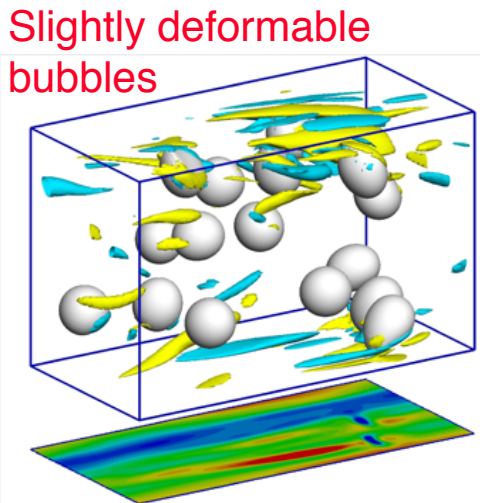
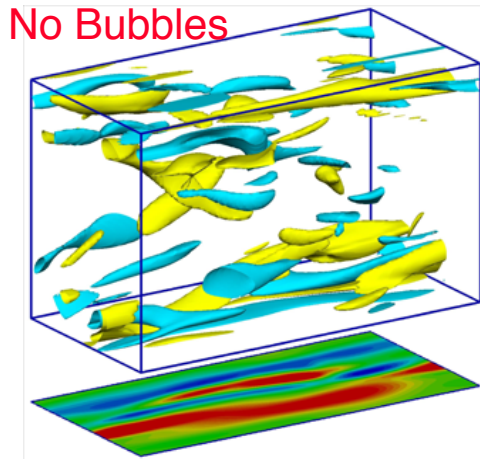
$$G(\vec{r}) = \frac{V}{N(N-1)} \left\langle \sum_i \sum_{j \neq i} \delta(\vec{r} - \vec{r}_{ij}) \right\rangle$$





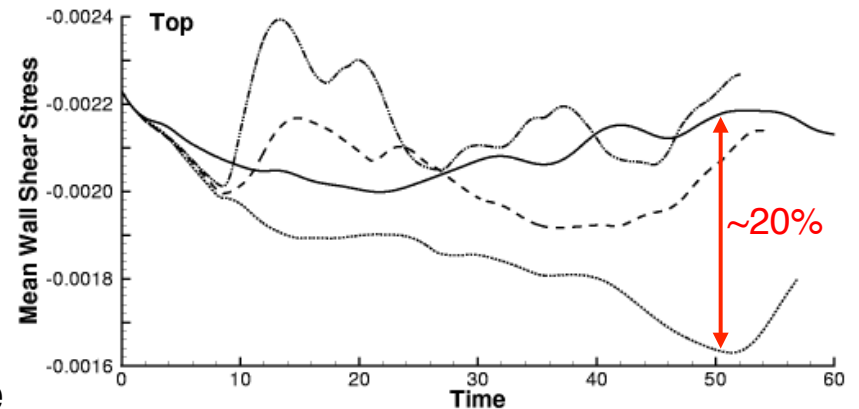
DNS of Multiphase Flows

Bubble Induced Drag Reduction



Experiment:
 $d^+=120$; $We=0.686$
Simulations:
 $d^+=54$; $We=0.203-0.405$

DNS of bubbles injected near the wall in a turbulent channel flow show that the deformability of the bubbles plays a major role. Bubbles with a deformability comparable to what is seen experimentally (S. L. Ceccio, taken in the LCC) can lead to drag significant drag reduction, but only for a short time. The simulations clarified the turbulent modification and showed that less deformable bubbles can lead to an increase in the wall drag.

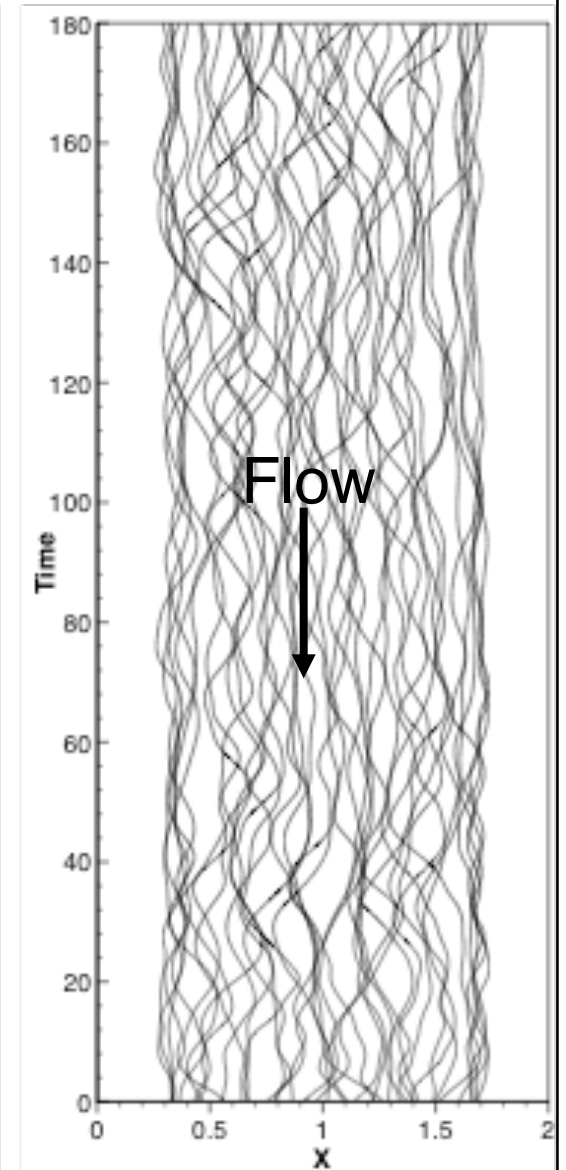
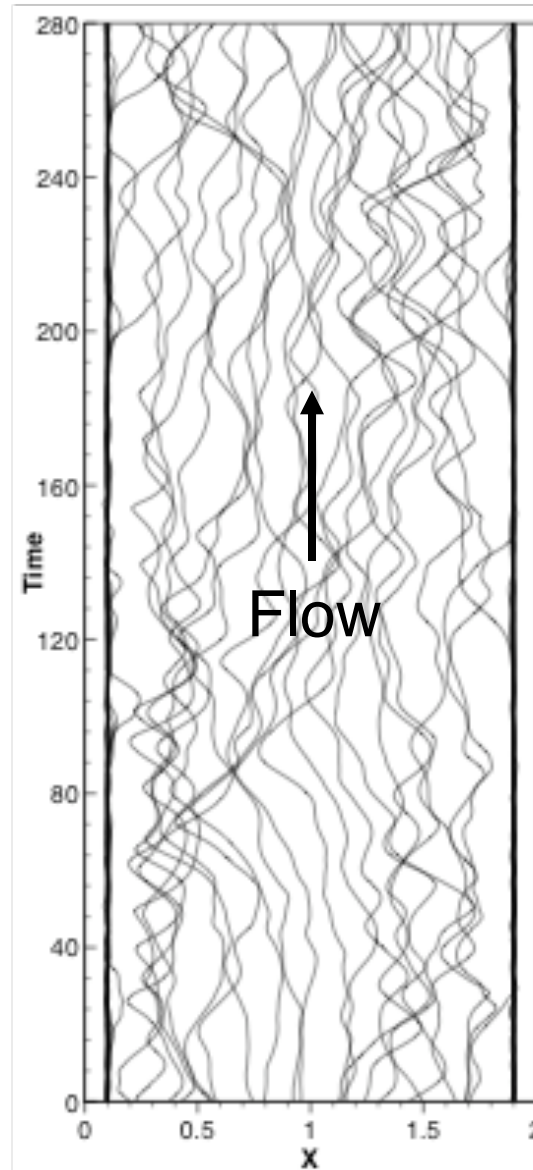
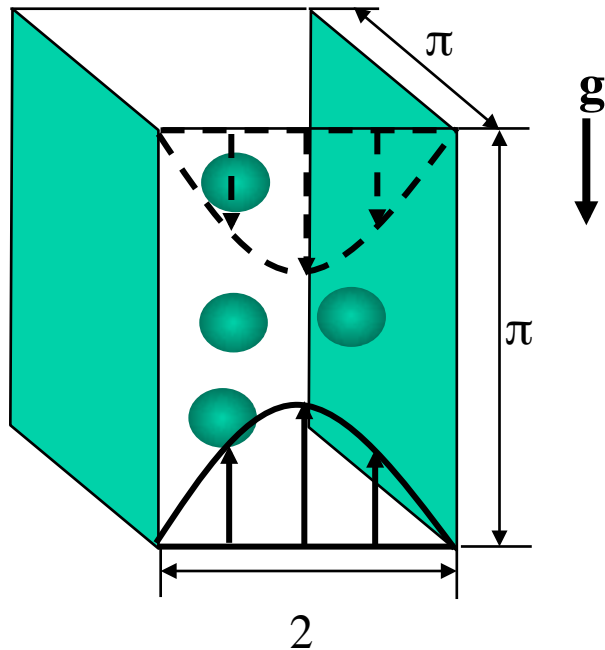




Bubbly Flows in Vertical Channels

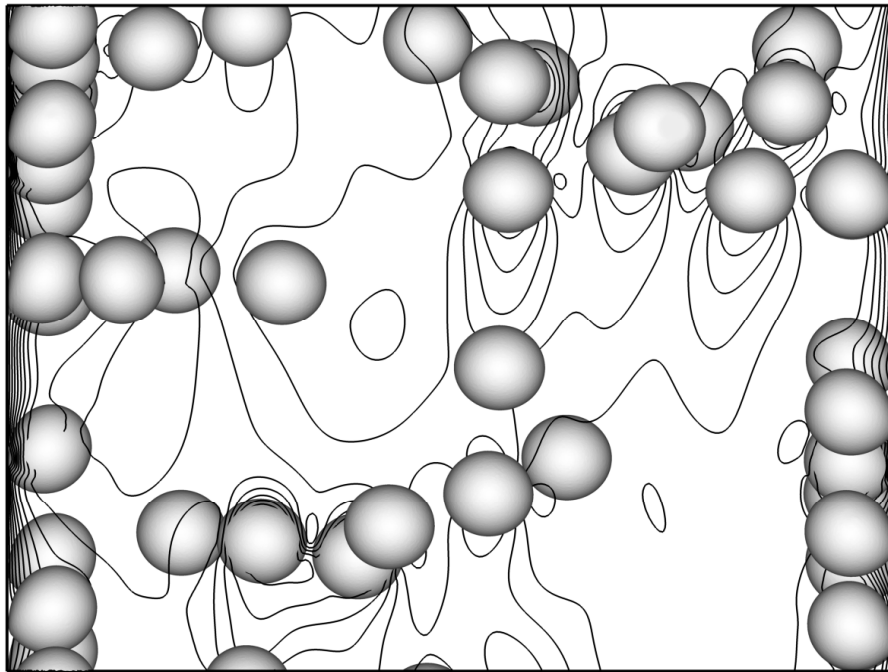
(with S. Biswas & J. Lu)

The path of bubbles. The cross-channel coordinate versus time for the upflow (left) and the downflow (right) at approximately steady state.

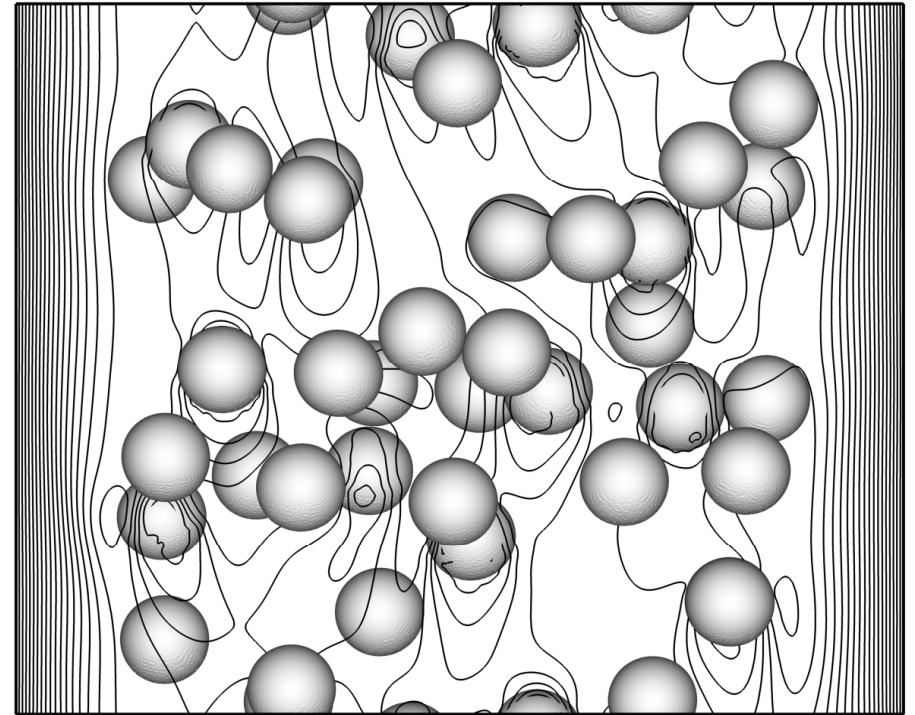


DNS of Multiphase Flows

Bubbles in Laminar Channel Flows



Upflow

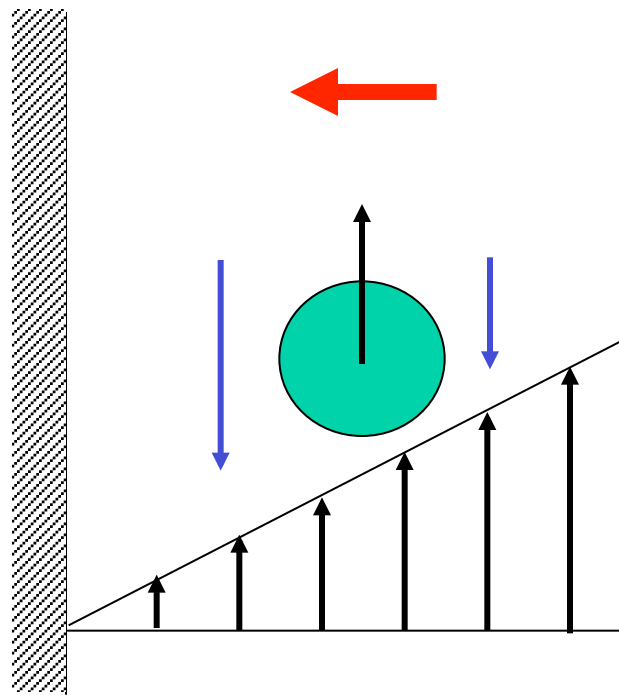


Downflow

The bubble distribution and isocontours of the vertical velocity in the middle plane for upflow on the left and downflow on the right. The velocity contours are plotted with 0.05 intervals.

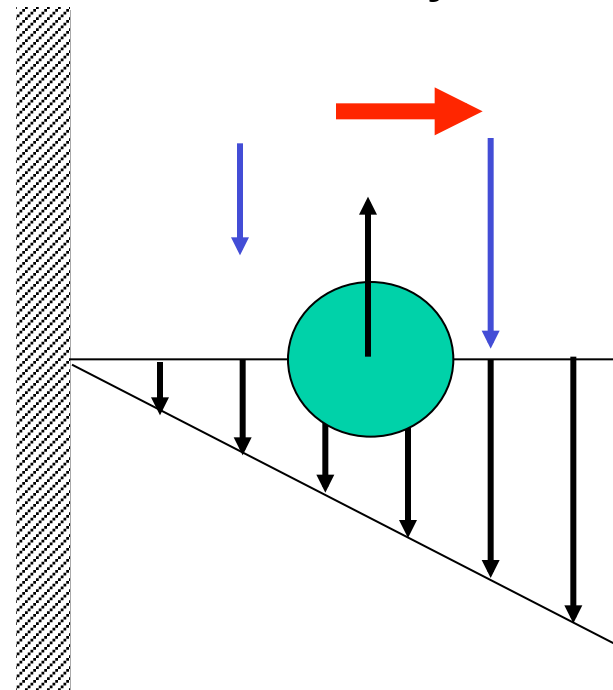
For a nearly spherical bubble

Lift toward wall



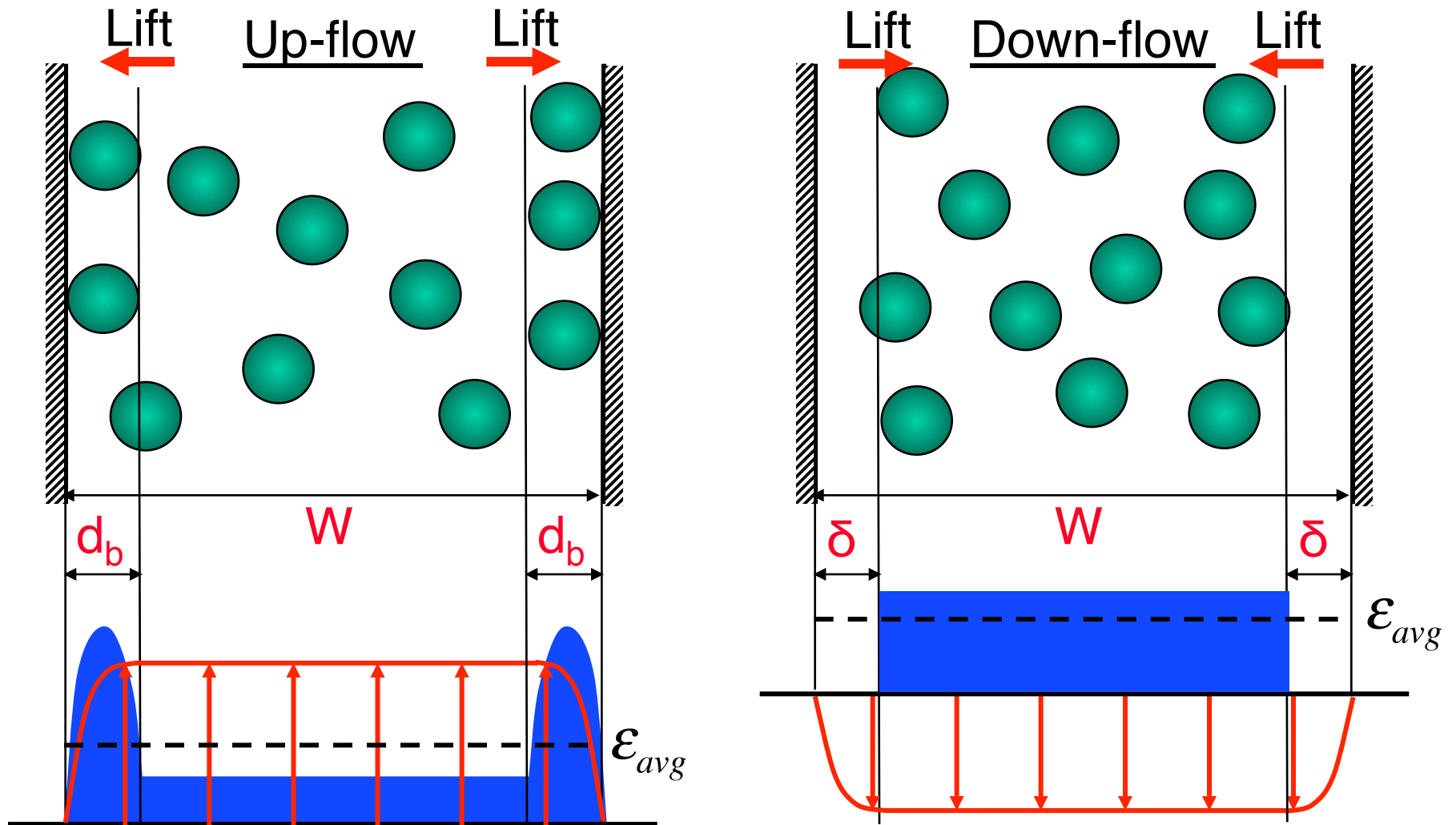
Upflow

Lift away from wall



Downflow

Simple two-fluid model for laminar multiphase flow

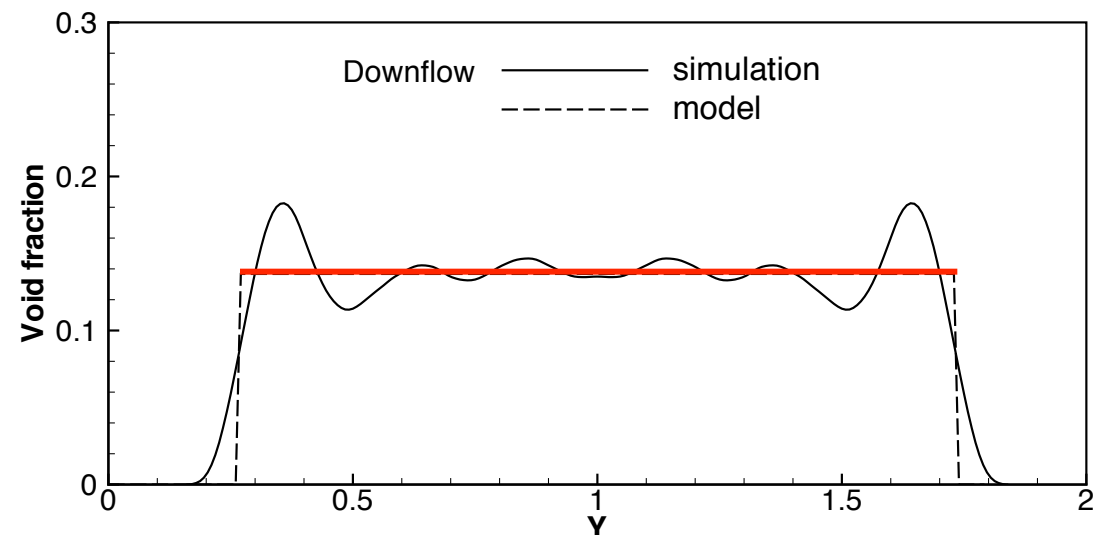
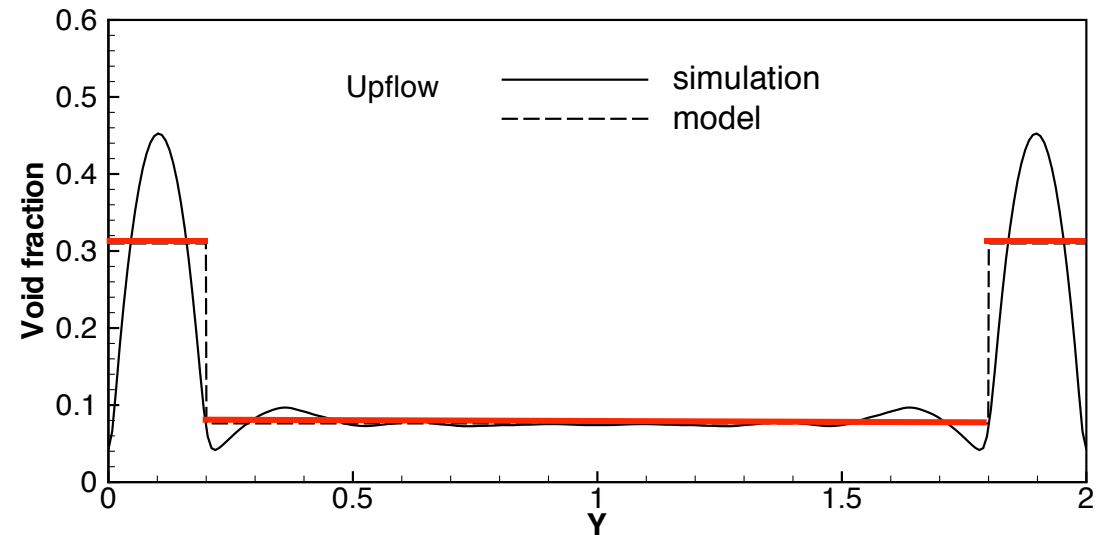




DNS of Multiphase Flows

Bubbles in Laminar Channel Flows

The average void fraction profile across the channel for the upflow (top) and the downflow (bottom). The solid lines denote the results from the simulations and the dashed lines are the analytical results.

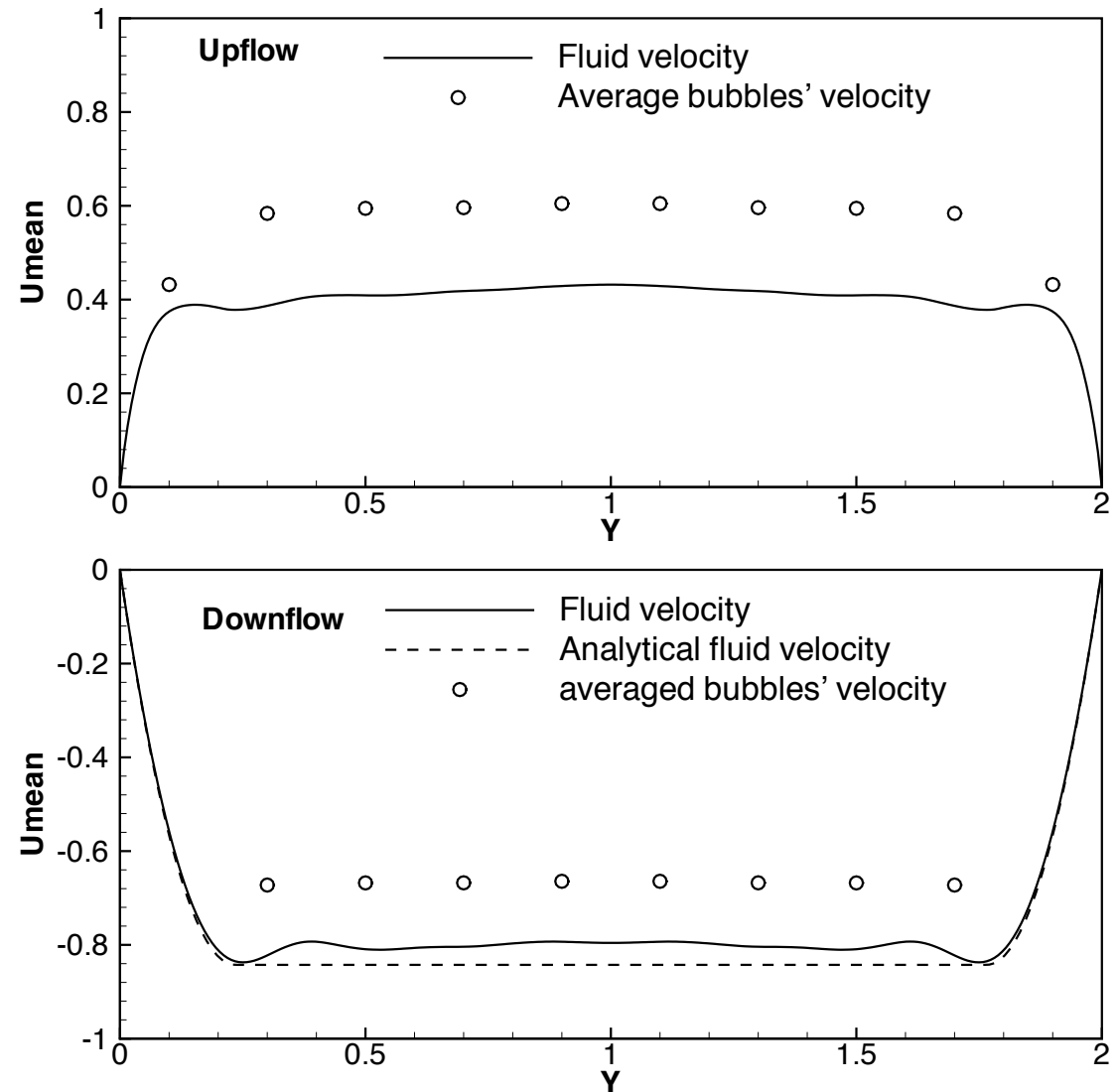




DNS of Multiphase Flows

Bubbles in Laminar Channel Flows

The average vertical liquid velocity profile across the channel for the upflow (top) and the downflow (bottom). The solid lines are the simulated results, averaged over 80 time units. The dashed line is the analytical results for the downflow. The circles represent the average bubble velocities in 10 equal sized bins across the channel.

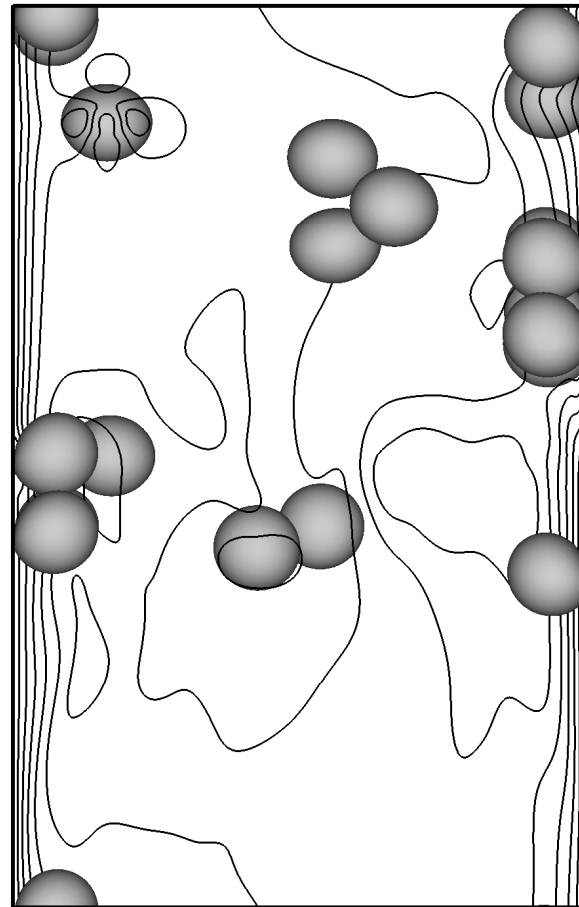




Effect of Bubble Deformability for Turbulent Upflow

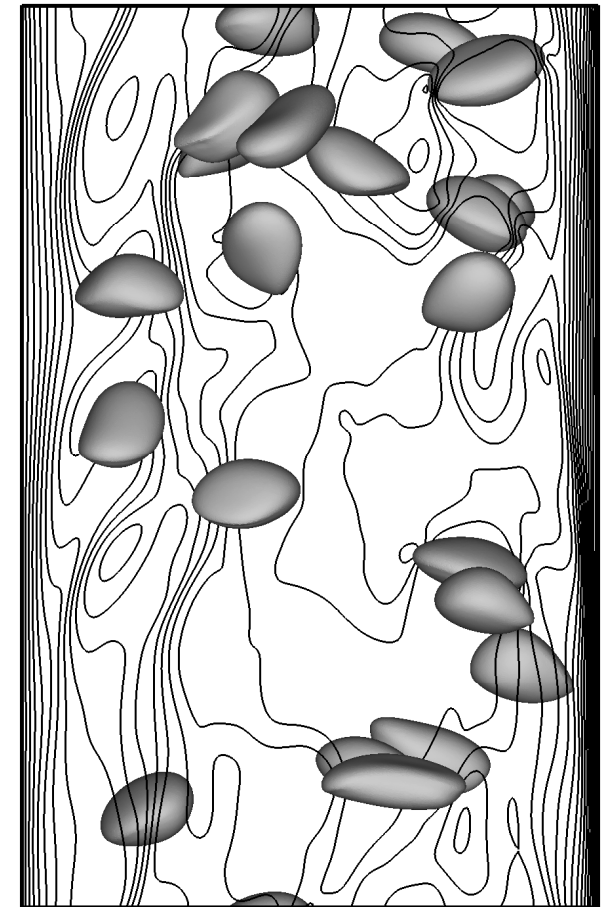
(with J. Lu)

The bubbles and iso-contours of the instantaneous vertical velocity in a plane through the middle of the channel for the upflow of nearly spherical (left) and much more deformable (right) bubbles at one time when the flow is approximately at steady state.



$$M=1.54 \times 10^{-10}$$

$$Eo=0.45$$



$$M=1.54 \times 10^{-7}$$

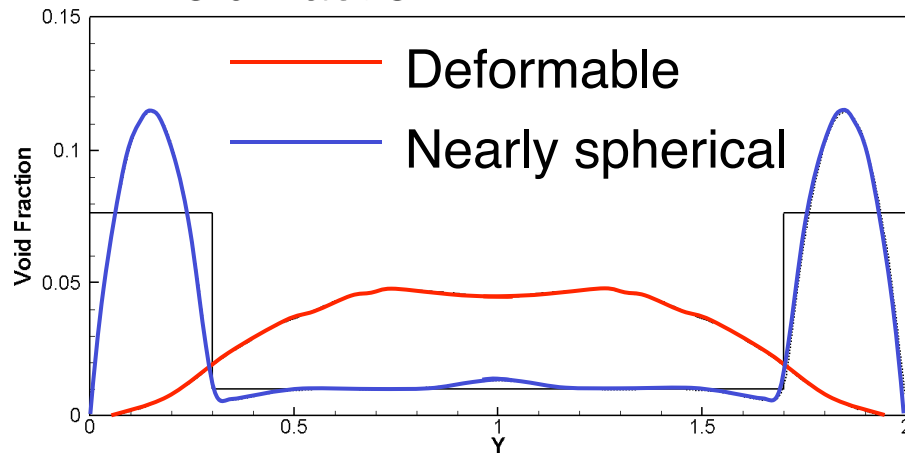
$$Eo=4.5$$



DNS of Multiphase Flows

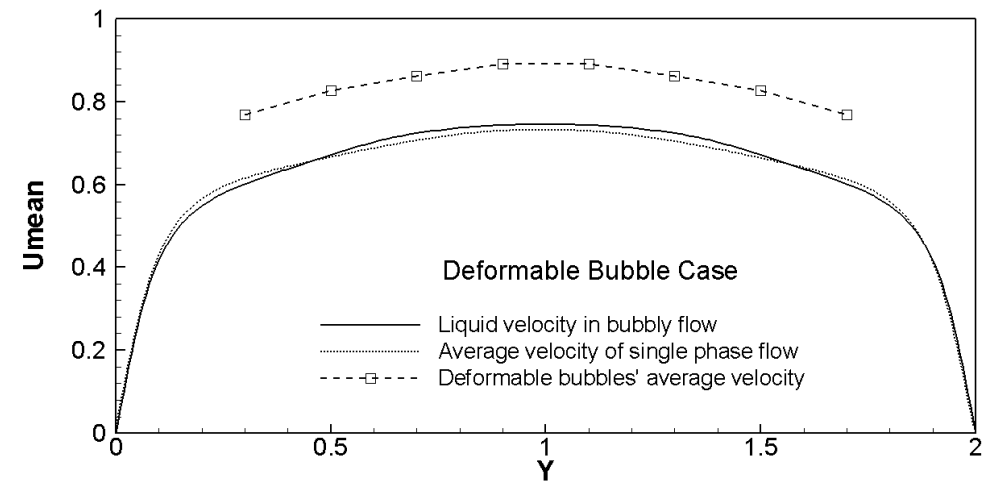
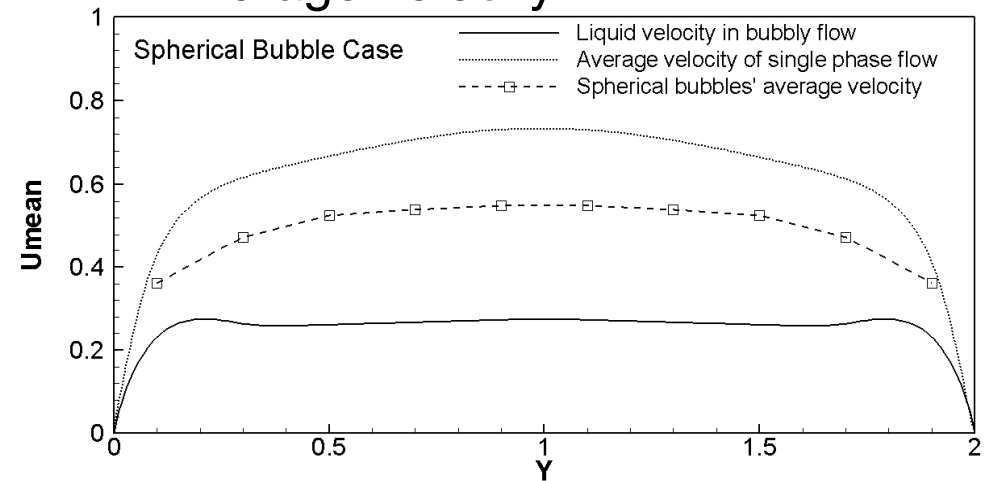
Turbulent Upflow: Effect of Deformability

Void fraction



The void fraction has major influence of the flow behavior. The void fraction is plotted above and the velocity profiles to the right, along with the velocity from flow without bubbles (rescaled to account for the change in average density). The wall peak in the void fraction for nearly spherical bubbles results in a reduction in the flow rate.

Average velocity



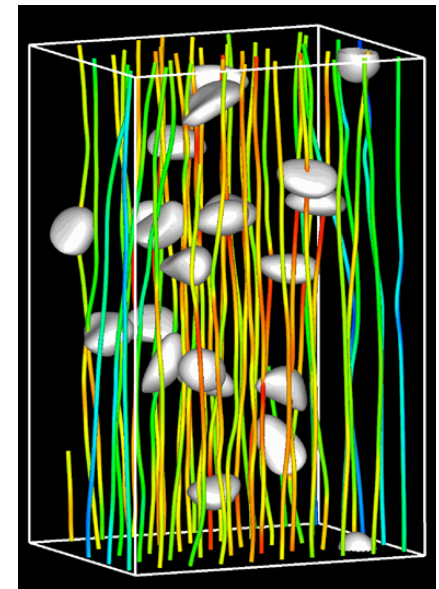
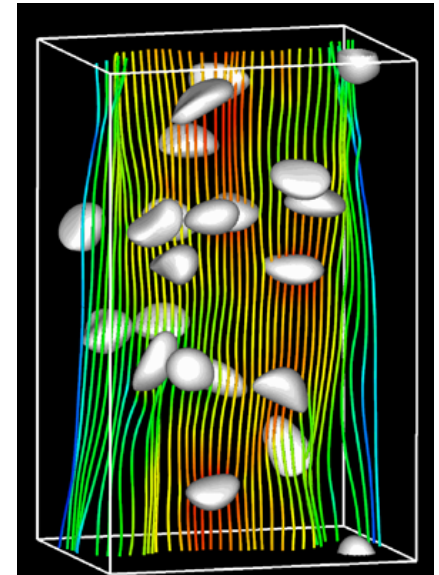
DNS of Multiphase Flows Bubbly flows in channels—Summary

For nearly spherical bubbles the flow consists of a homogeneous core where the mixture is in hydrostatic equilibrium and a wall-layer.

For upflow the wall-layer is bubble rich and the total flow rate depends strongly on the deformability of the bubbles.

For downflow the wall-layer has no bubbles and the velocity profile is easily found for both laminar and turbulent flow. For downflow the exact size of the bubbles plays only a minor role, as long as they remain nearly spherical.

For upflow deformable bubbles stay away from walls, completely changing the flow structure





Additional Fields & Forces Temperature & Electricity



Thermocapillary migration

The temperature is found by solving the energy equation

$$\frac{\partial \rho c_p T}{\partial t} + \nabla \cdot (\rho c_p T \mathbf{u}) = \nabla \cdot k \nabla T$$

The temperature on the surface of the bubble or drop is found by interpolating it from the grid and surface tension is found by $\sigma = \sigma_o - \beta(T - T_o)$

Electrohydrodynamics of suspensions

The electric field is obtained from the equation for the conservation of current:

$$\frac{Dq}{Dt} = \nabla \cdot \sigma \mathbf{E}$$

neglecting the convection of charge

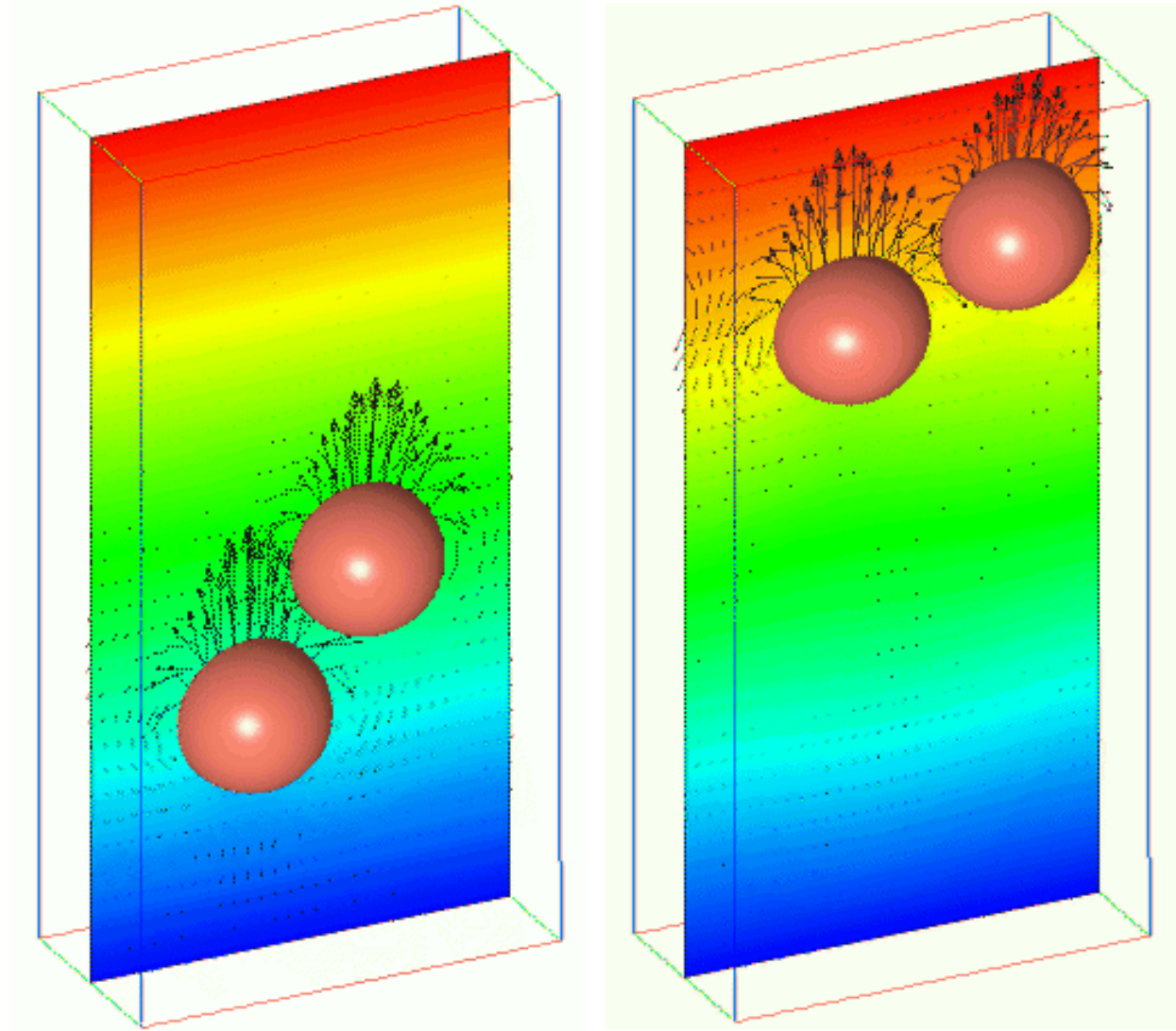
the charge accumulation is found by:

$$q = \nabla \cdot \epsilon \mathbf{E}$$

The force on the fluid is then found by:

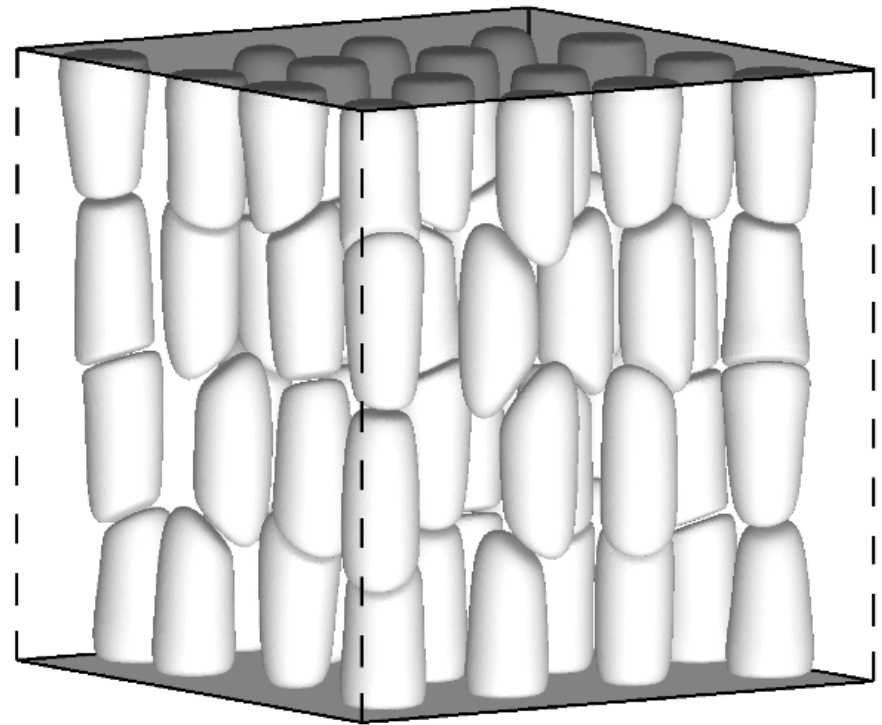
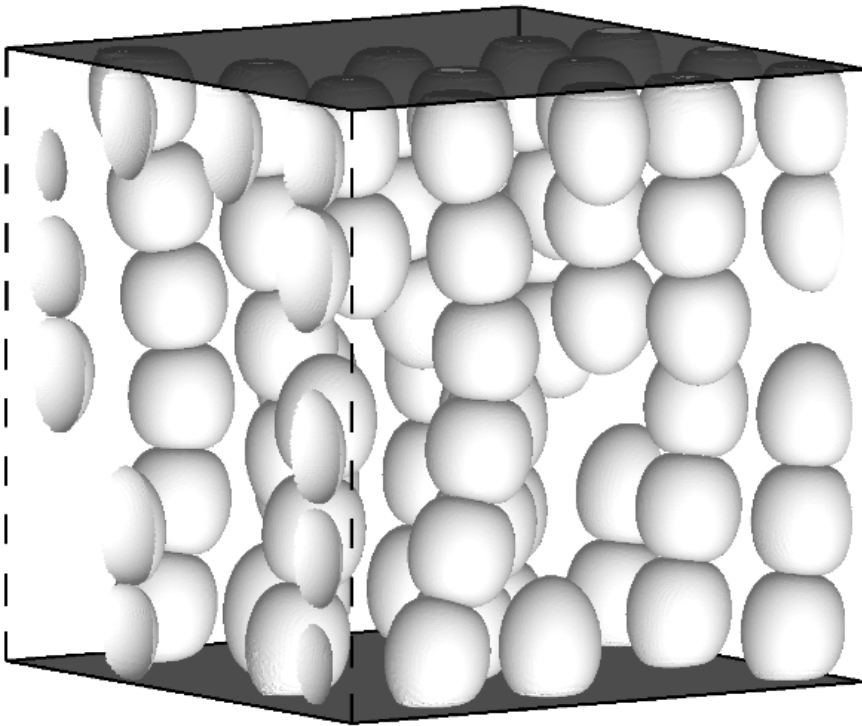
$$\mathbf{f} = q \mathbf{E} - \frac{1}{2} (\mathbf{E} \cdot \mathbf{E}) \nabla \epsilon$$

Thermocapillary motion of two three-dimensional bubbles. The top wall is hot and the bottom wall is cold. Initially the bubbles are placed near the cold wall. As they rise, the bubbles line up perpendicular to the temperature gradient.



$$\begin{aligned}\sigma_i/\sigma_o &= 0.005 & \text{Re} &= 20 \\ \varepsilon_i/\varepsilon_o &= 0.01 & \text{We} &= 0.0625 \\ \alpha &= 20\% & E^* &= 0.0182\end{aligned}$$

$$\begin{aligned}\sigma_i/\sigma_o &= 0.01 & \text{Re} &= 20 \\ \varepsilon_i/\varepsilon_o &= 0.1 & \text{We} &= 0.0625 \\ \alpha &= 20\% & E^* &= 0.04\end{aligned}$$





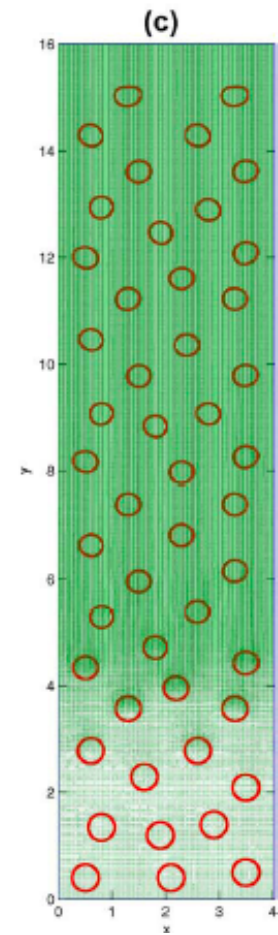
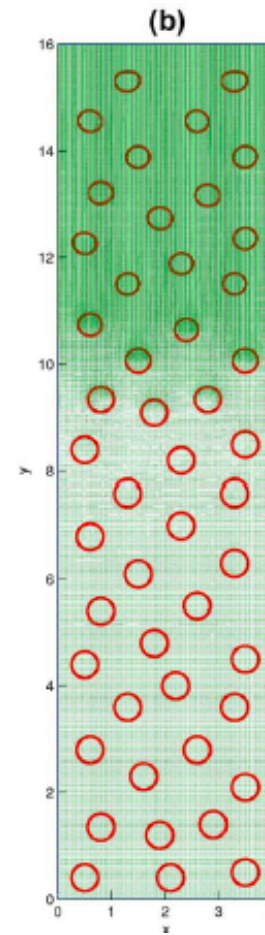
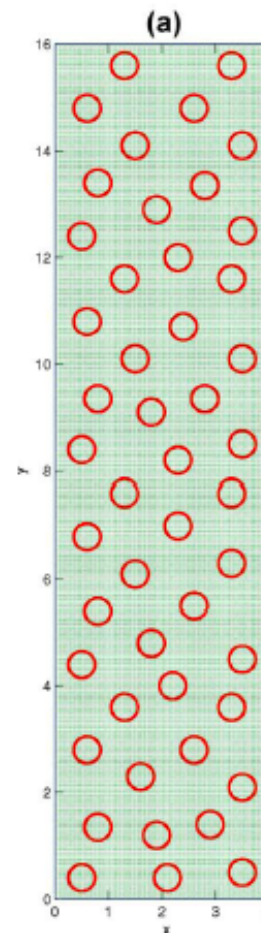
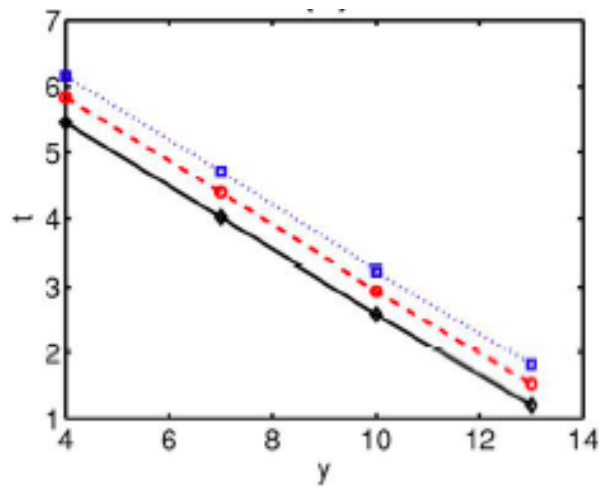
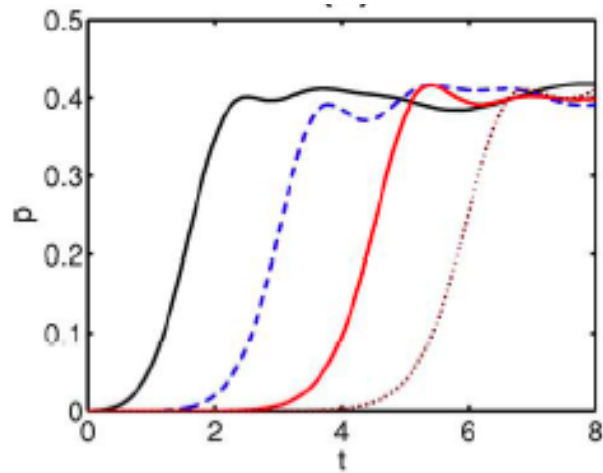
Cavitating Bubbly Clouds



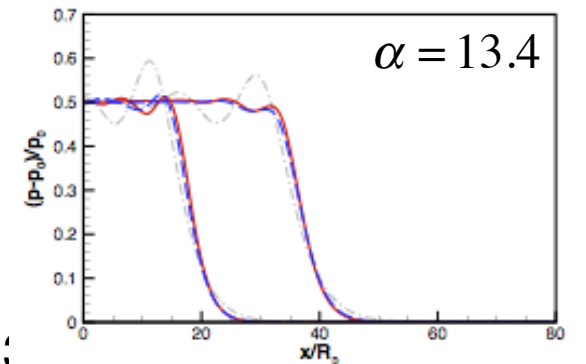
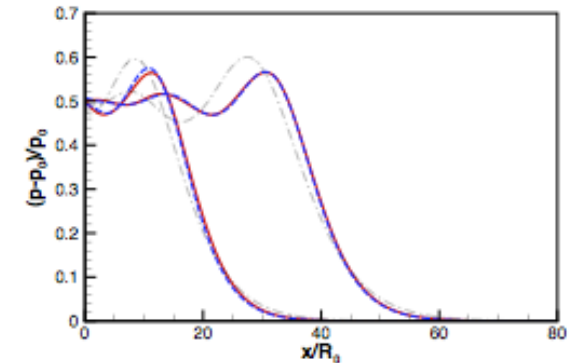
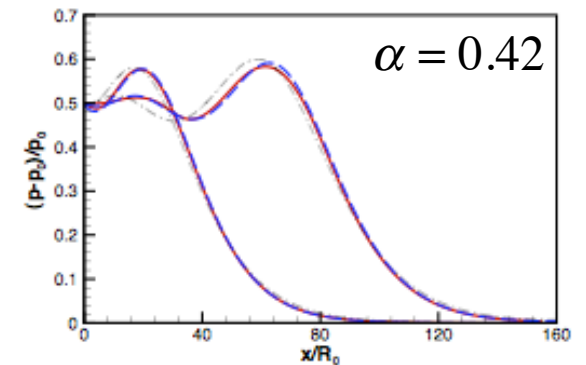
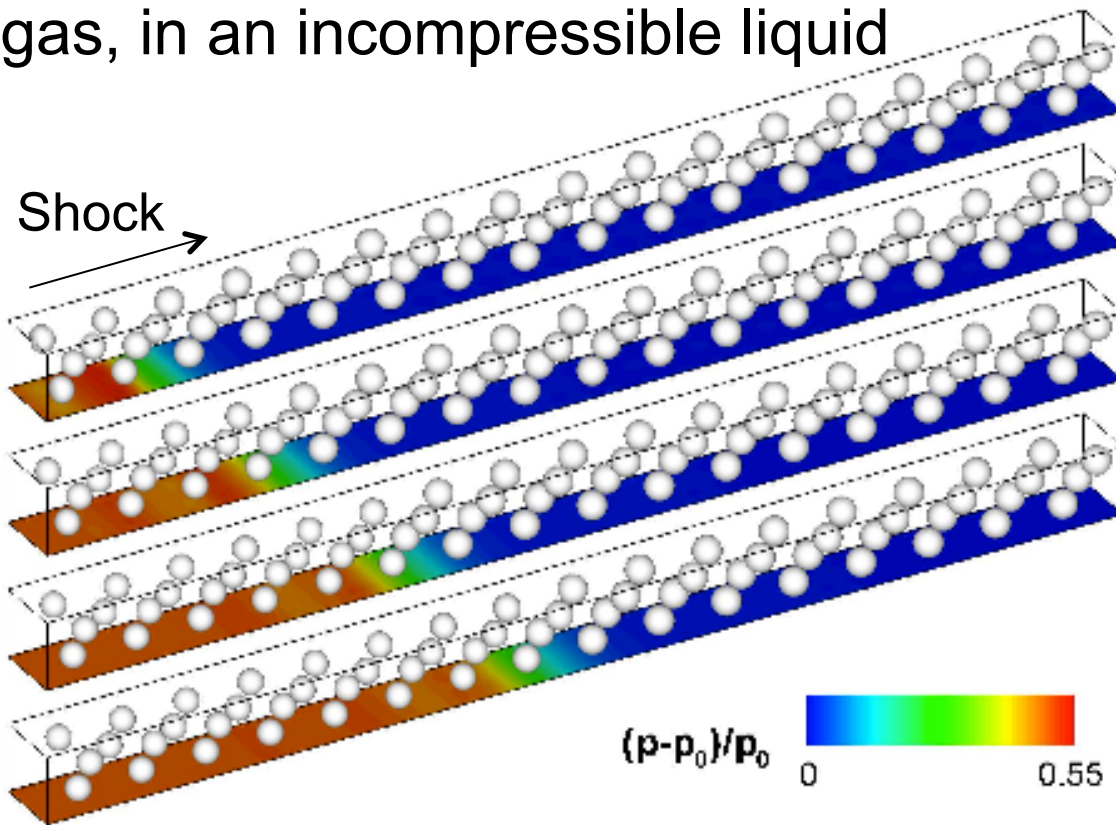
DNS of Multiphase Flows

Shocks in bubbly liquid

Polytropic gas inside the bubbles



Compressible bubbles filled with ideal gas, in an incompressible liquid



C.F. Delale and G. Tryggvason. "Shock structure in bubbly liquids: Comparison of Direct Numerical Simulations and model equations." *Shock Waves* 17 (2008), 433–440.

J. H. Seo, S. K. Lele and G. Tryggvason. "Investigation and modeling of bubble-bubble interactions effect in homogeneous bubbly flows." *Physics of Fluids*, in press



Simulations of Boiling Flows

(with D. Juric, A. Esmaeeli & J. Lu)



DNS of Multiphase Flows

Governing Equations

$$\rho \frac{\partial \mathbf{u}}{\partial t} + \rho \nabla \cdot \mathbf{u} \mathbf{u} = -\nabla p + \mathbf{f} + \nabla \cdot \mu (\nabla \mathbf{u} + \nabla^T \mathbf{u}) + \int_F \sigma \kappa \mathbf{n} \delta(\mathbf{x} - \mathbf{x}_f) da$$

$$\frac{\partial cT}{\partial t} + \mathbf{u} \cdot \nabla cT = \nabla \cdot k \nabla T + \int \dot{q} \delta(\mathbf{x} - \mathbf{x}_f) dA \quad \text{Energy equation}$$

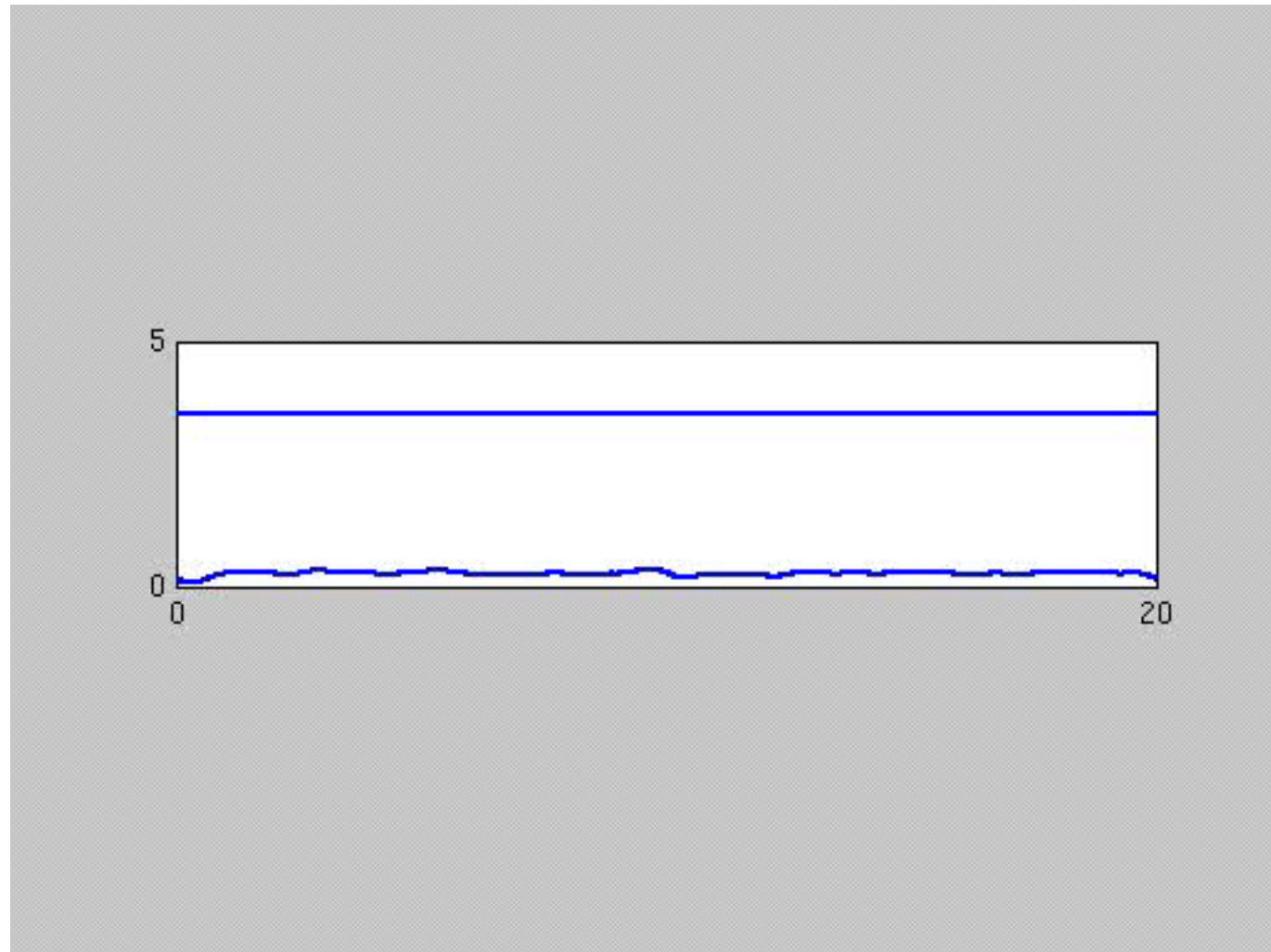
$$\dot{q} = k_1 \left. \frac{\partial T}{\partial n} \right|_1 - k_2 \left. \frac{\partial T}{\partial n} \right|_2 \quad \text{Heat source}$$

$$T_l = T_v = T_{sat}(p_{sys}) \quad \text{Thermodynamic}$$

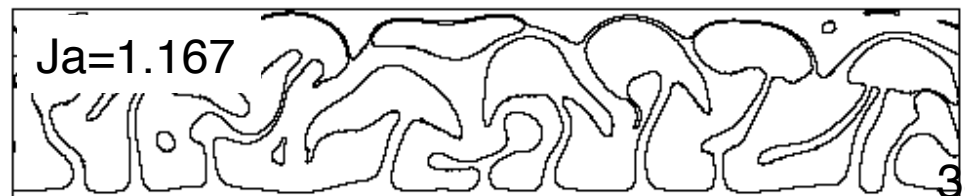
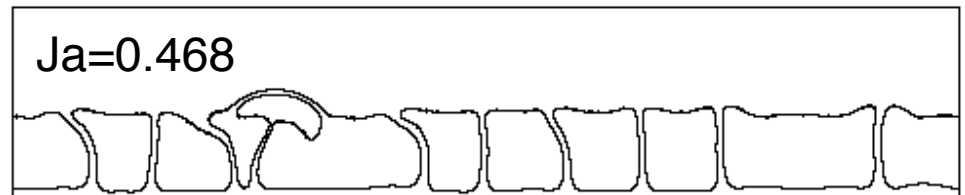
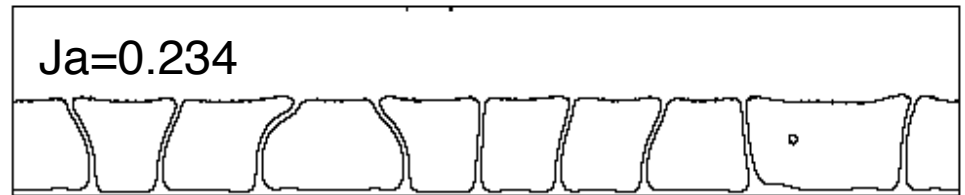
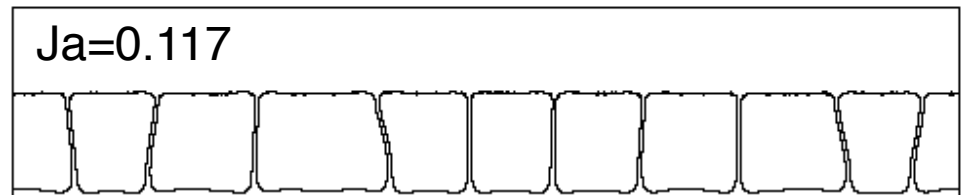
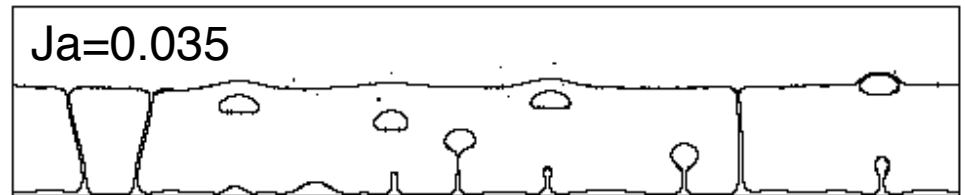
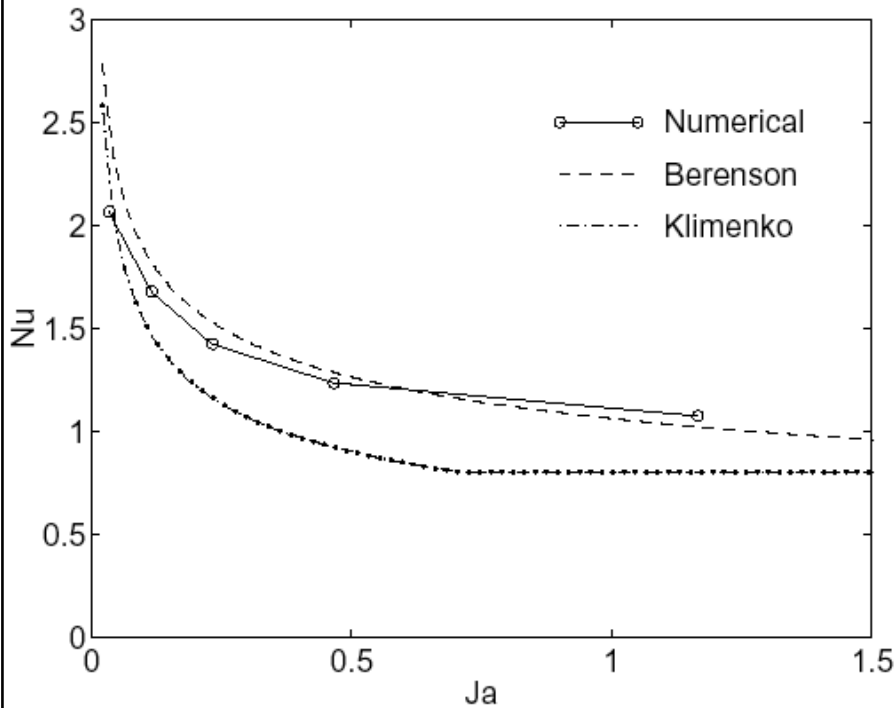
$$\nabla \cdot \mathbf{u} = \frac{1}{L} \left(\frac{1}{\rho_v} - \frac{1}{\rho_f} \right) \int \dot{q} \delta(\mathbf{x} - \mathbf{x}_f) dA \quad \text{Mass conservation}$$

$$V_n = \frac{1}{2} (u_l + u_v) - \frac{\dot{q}}{L} \left(\frac{1}{\rho_v} + \frac{1}{\rho_f} \right) \quad \left. \vphantom{\frac{1}{2}} \right\} \text{Velocity of bdry}$$

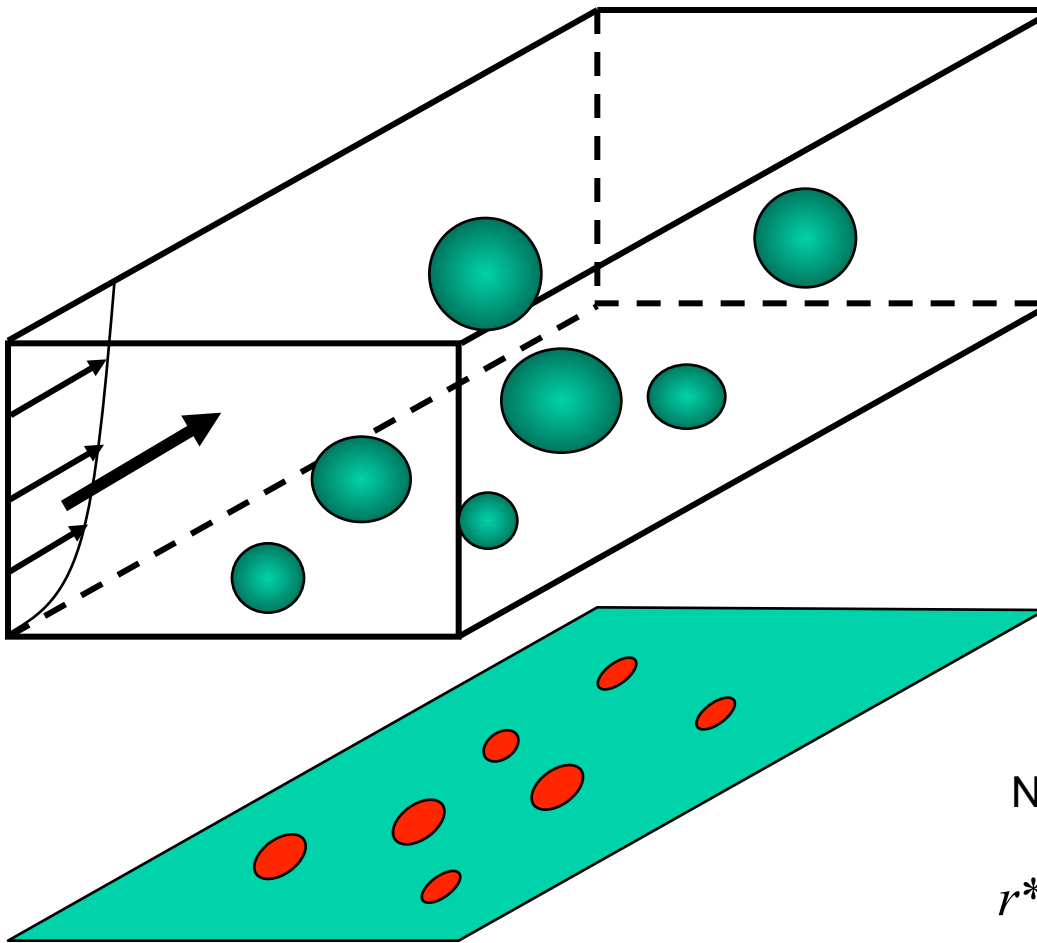
$$\frac{d\mathbf{x}_f}{dt} = V_n \mathbf{n} + \mathbf{u}$$



The effect of the Jacob number on the boiling for near critical film boiling



Nucleate Flow Boiling



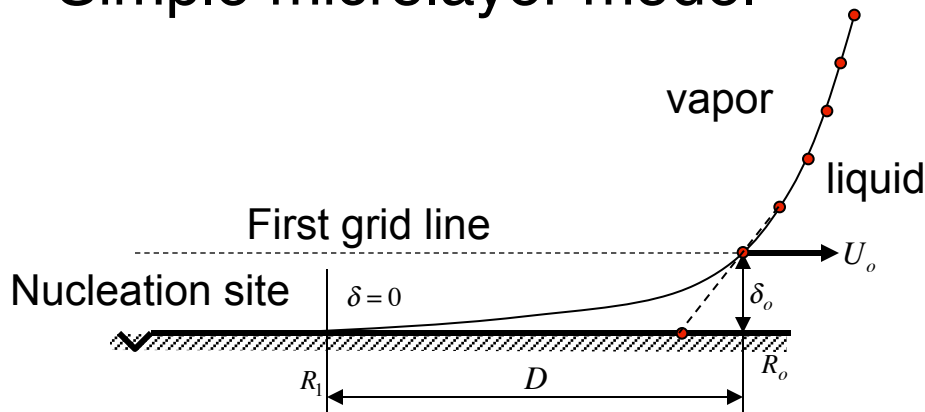
Assumption : Surface nucleation characteristics determined by size distribution of potentially active sites

- Random spatial site distribution
- Random conical cavity size (mouth radius, r) distribution
- Assume vapor embryo radius = r
- Assume near wall liquid film is stationary

Nucleation site is active if $r_{\min} > r^*$

$$r^* = \frac{2\sigma T_{sat} \nu_{lv}}{h_{lv} [T_l - T_{sat}]} \quad \text{Carey (1992)}$$

Simple microlayer model



Evaporation of the film

$$\dot{q} = k \frac{T_w - T_f}{\delta} = k \frac{\Delta T}{\delta} \quad \text{Heat transfer}$$

$$\frac{d\delta}{dt} = -\frac{\dot{q}}{\rho_f L} = -\frac{k\Delta T}{\delta \rho_f L} = -\frac{\beta}{\delta} \quad \text{Evaporation}$$

$$\delta = \sqrt{\delta_o^2 - 2\beta t} \quad \text{Integrate to find thickness}$$

$$t_e = \delta_o^2 / 2\beta$$

$$D = U_o t_e = \frac{U_o \delta_o^2}{2\beta} \quad \text{Find length of film}$$

Total heat transfer to the microlayer

$$\dot{Q} = \int_0^D \dot{q} dx = \int_0^D \frac{k\Delta T}{\sqrt{\delta_o^2 - (2\beta/U_o)x}} dx = \frac{k\Delta T}{\delta_o} \int_0^D \frac{1}{\sqrt{1 - (2\beta/\delta_o^2 U_o)x}} dx \quad \rightarrow \quad \dot{Q} = \delta_o U_o L \rho_f$$

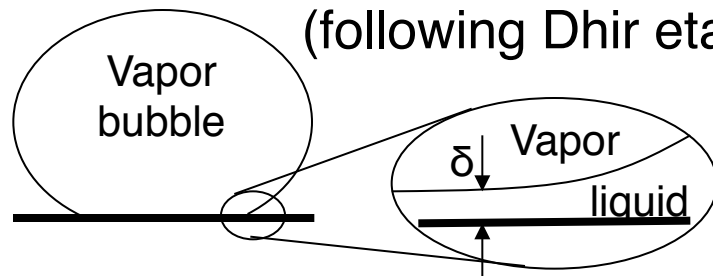
Volume expansion

$$\dot{V} = \frac{\dot{Q}}{L} \left(\frac{1}{\rho_v} - \frac{1}{\rho_f} \right)$$

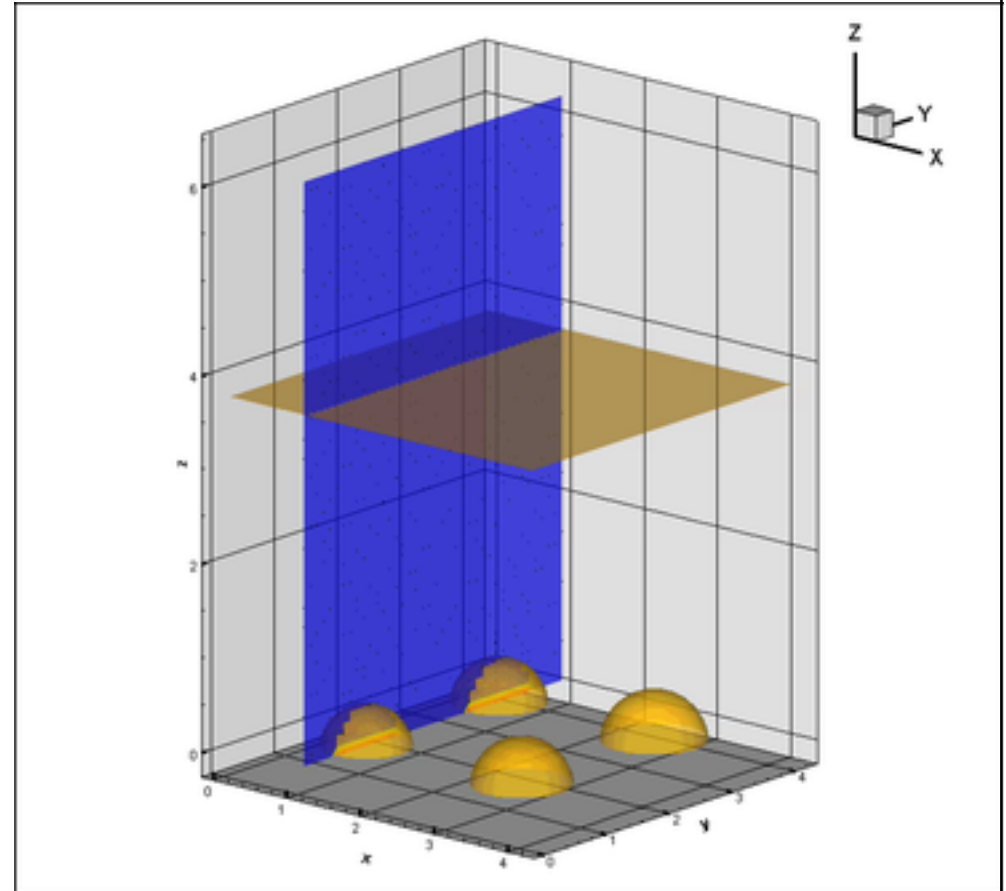
Applied near the apparent contact

Simulation of the generation of bubbles in a shallow pool. In addition to solving the energy equation, the latent heat and the volume expansion at the phase boundary must be included. Most simulations so far have been for film boiling. The nucleation of a vapor bubble and the evaporation in the microlayer must be addressed by multiscale modeling.

Microlayer modeling (following Dhir et al)



Movie from D. Juric



Water at 1atm, $T_{sat}=373.15K$; liquid/vapor density ratio=1605; viscosity ratio=23; thermal conductivity ratio=27; specific heat ratio=1; domain size: 10.5x10.5x15.75 mm; Wall superheat: 18K
40x40x60 grid resolution

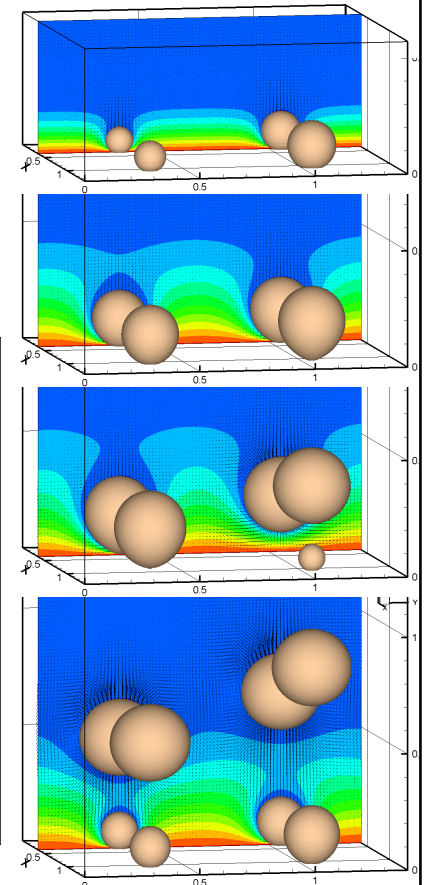
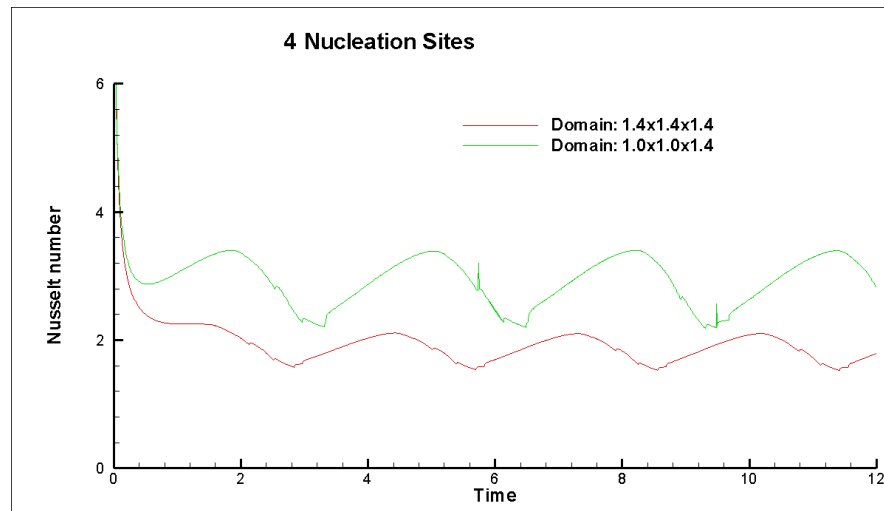
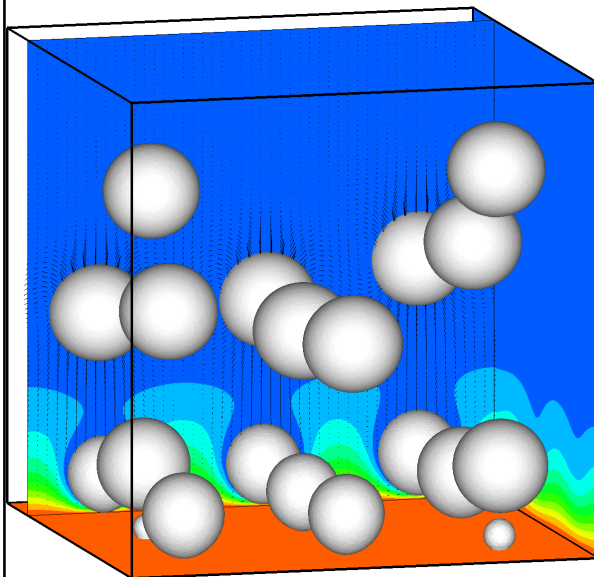
DNS of Multiphase Flows

Nucleate Boiling

There appears to be no significant technical obstacles for conducting large scale simulations of nucleate flow boiling—however, some development works still needs to be done!

Such simulations should allow us to

- Assess the accuracy of the assumptions made in the modeling of the microlayer
- Use the simulations to make predictions about boiling under conditions where experiments are difficult or do not yield the necessary data.





DNS of Multiphase Flows
DNS with multi-scale models

Multiphase flow DNS with embedded multi-scale models

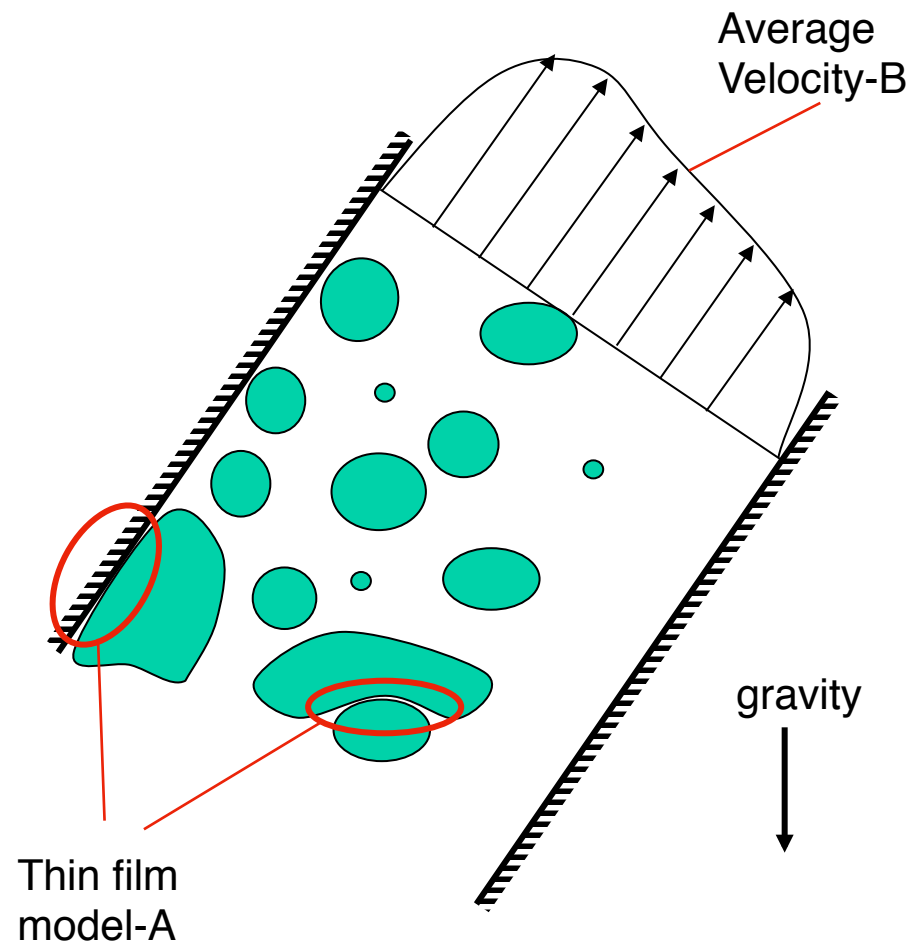
Some communities have defined two types of multi-scale problems.

Type A Problems: Dealing with Isolated Defects

Type B Problems: Constitutive Modeling Based on the Microscopic Models

Reference: W. E and B. Enquist, The heterogeneous multiscale methods, *Comm. Math. Sci.* **1** (2003), 87—133.

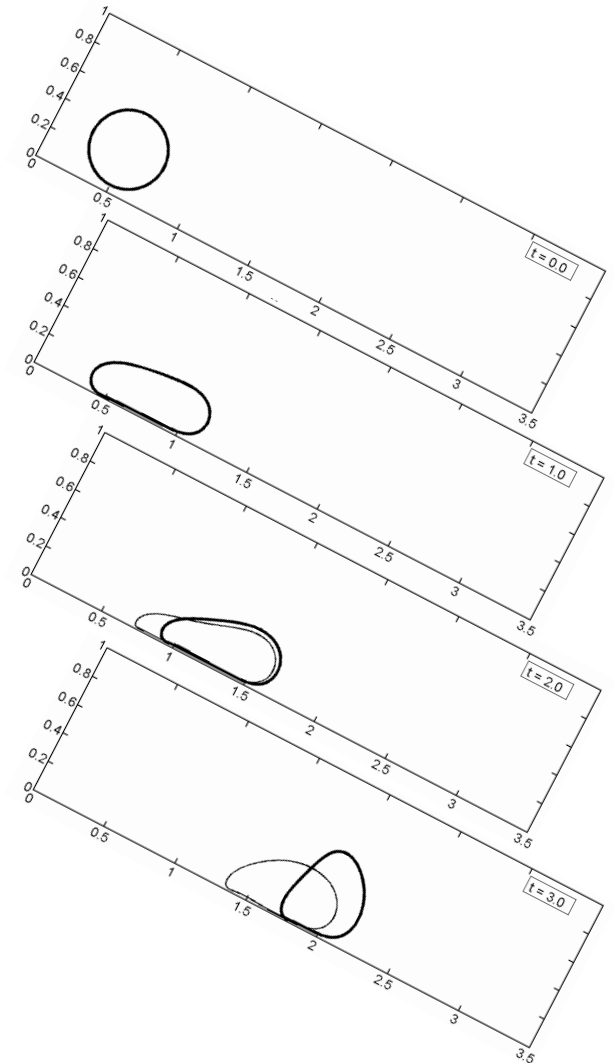
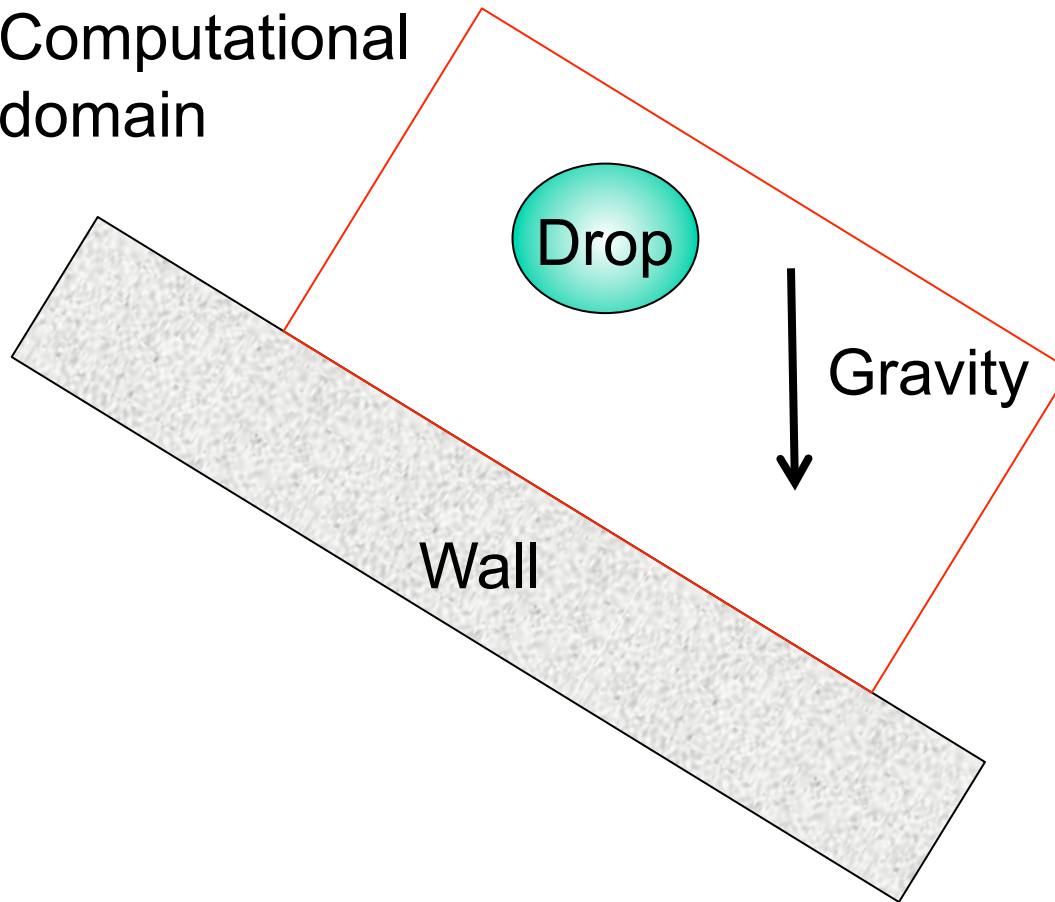
Buoyant bubbles in an inclined channel flow



DNS of Multiphase Flows

DNS with multi-scale models

Computational domain

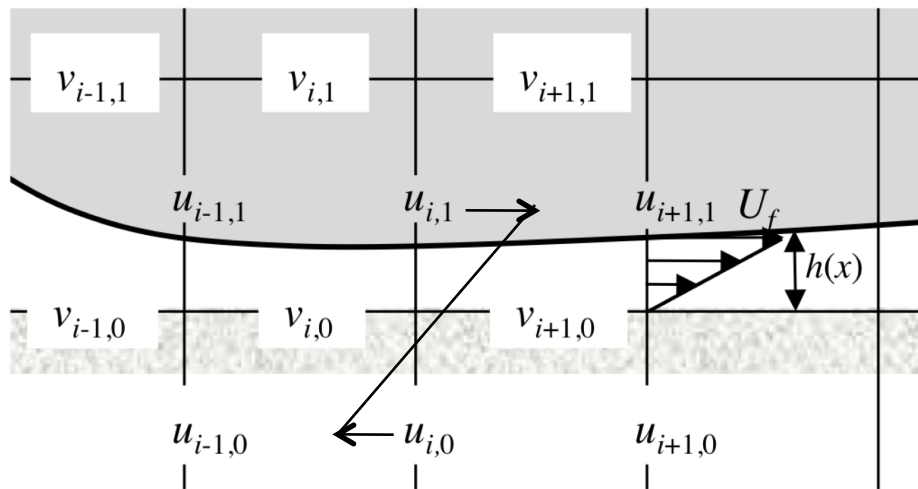


S. Thomas, A. Esmarelli and G. Tryggvason. "Multiscale computations of thin films in multiphase flows." *Int'l J. Multiphase Flow* 36 (2010), 71-77.

Film model—linear velocity profile

$$\frac{\partial h}{\partial t} + \frac{1}{2} \frac{\partial}{\partial x} (hU_f) = 0;$$

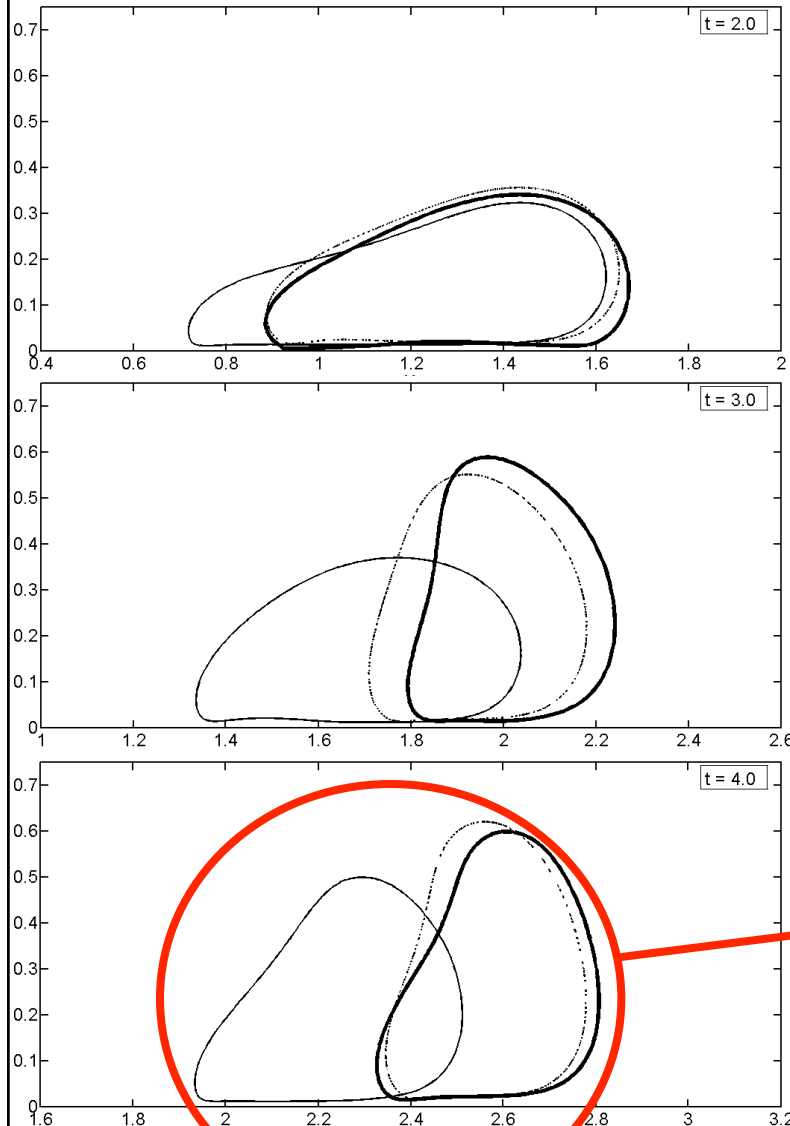
$$\frac{\partial}{\partial t} (hU_f) + \frac{2}{3} \frac{\partial}{\partial x} (hU_f^2) = - \frac{2h}{\rho_o} \left(\frac{dp}{dx} \right)_f,$$



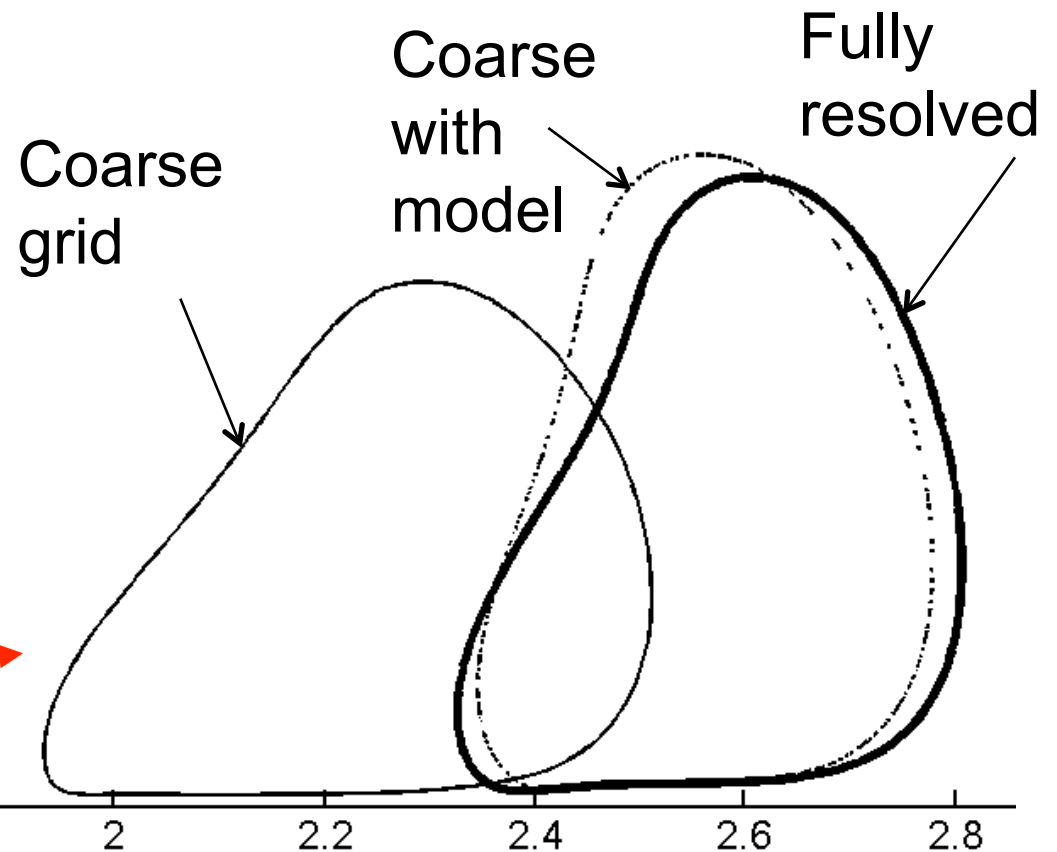
Wall shear and ghost velocity:

$$\tau_f = \mu_o \frac{U_f}{h} \Rightarrow u_{i,0} = u_{i,1} - \frac{\tau_f \Delta y}{\mu_d}$$

1. Identify whether a grid points at a wall belong to a film or not.
2. For film wall-points, given h and U_f , find the wall-shear and set the ghost velocities. For points outside the film, use the no-slip boundary condition.
3. Solve the Navier-Stokes equations for the velocity and pressure at the next time step, using the ghost velocities set above.
4. Integrate the thin film equations, using the pressure at the wall as computed by solving the Navier-Stokes equations (step 3).
5. Go back to (1)



Drop motion on a sloping wall.
Impact of fully resolving the film
between the drop and the wall



Computations of chemical reactions in bubble wakes



A-liquid reactant,
 B-gaseous reactant,
 R-desired product,
 S-impurity.

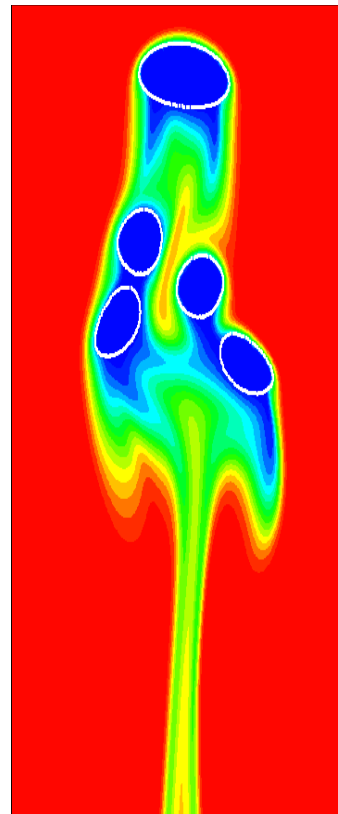
Re=20, based on the large bubble;
 bubble diameter ratio – 1:1.4;
 Sc=300,
 Da₁=0.25 and Da₂=0.025

Dimensionless reaction rates:

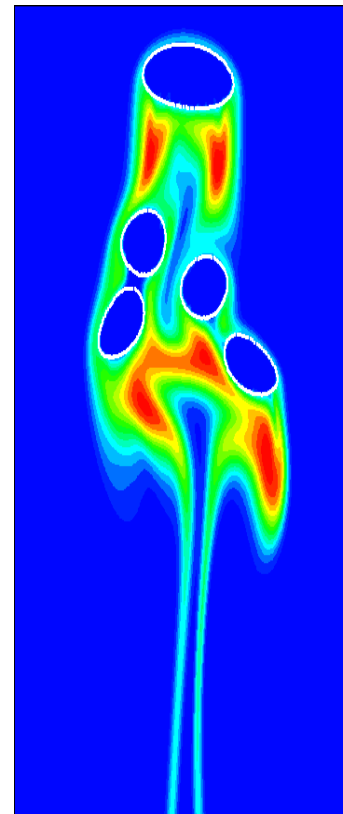
$$r_1 = Da_1 \cdot c_A \cdot c_B$$

$$r_2 = Da_2 \cdot c_A \cdot c_R$$

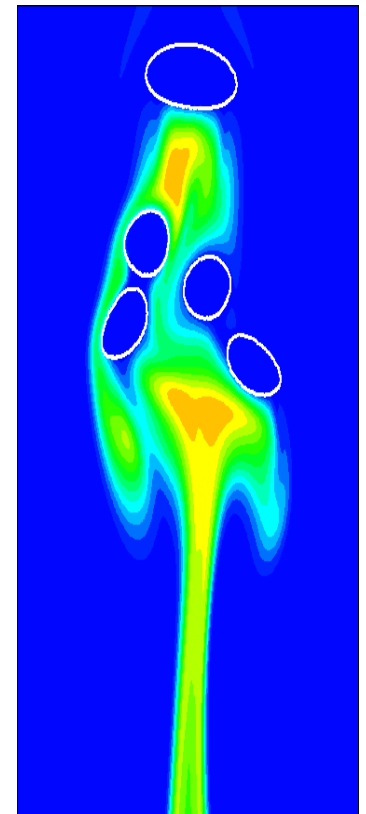
liquid-phase
reactant



desired
product

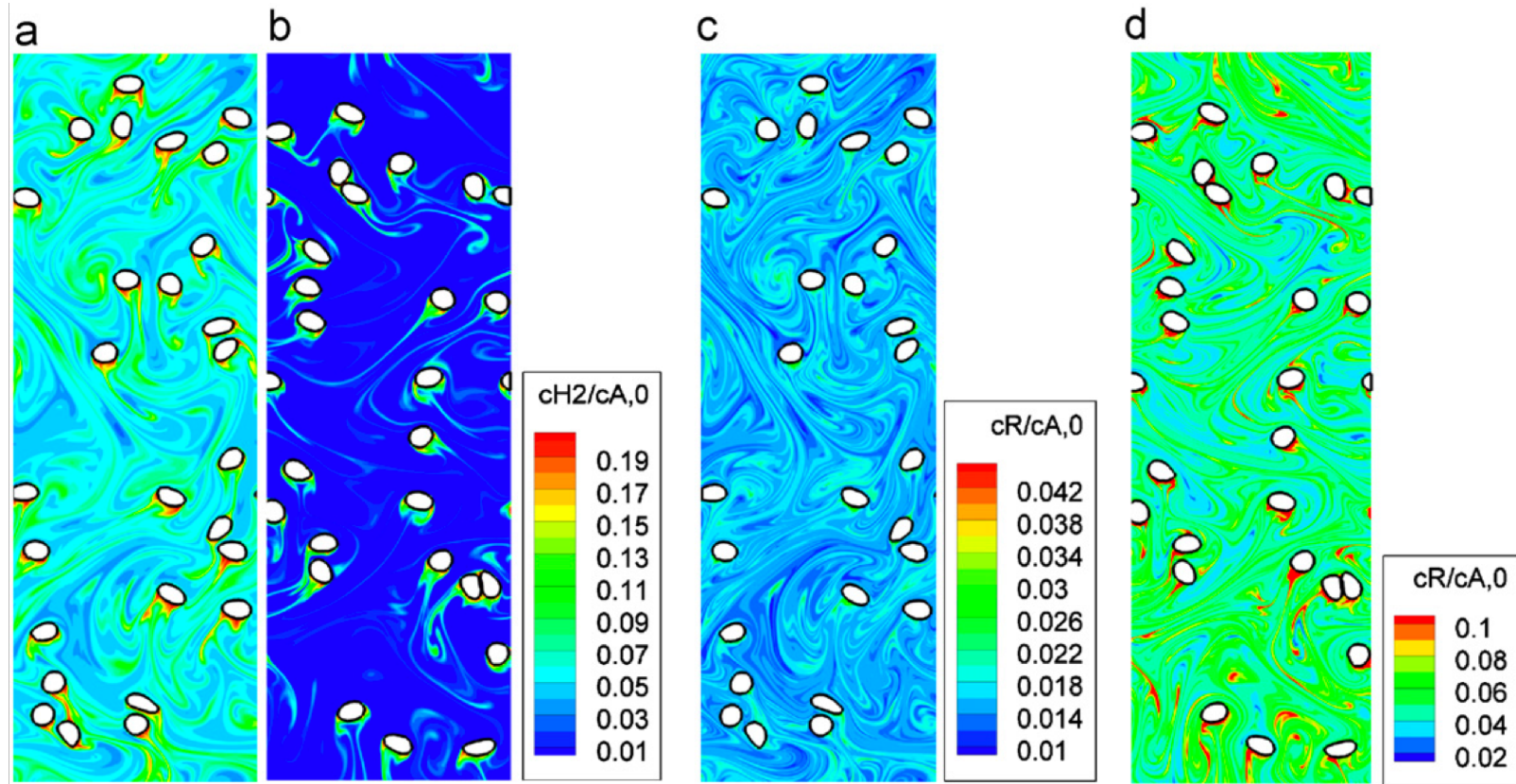


by-
product

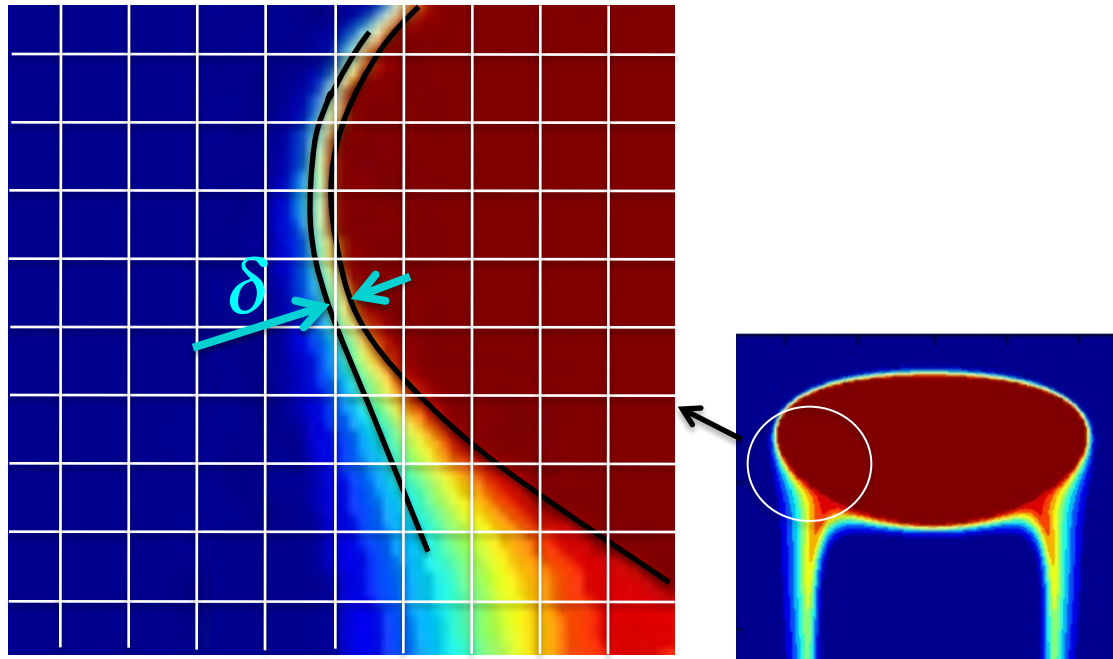


A. Koynov, G. Tryggvason, and J. G. Khinast. "Mass Transfer and Chemical Reactions in Bubble Swarms with Dynamic Interfaces." *AIChE Journal* 10 (2005), 2786-2800.

A. Koynov, G. Tryggvason, M. Schlüter, J. G. Khinast. "Mass Transfer and Chemical Reactions in Reactive Deformable Bubble Swarms." *Appl. Phys. Lett.* 88, 134102 (2006)



Results from simulations of the catalytic hydrogenation of nitroarenes. The hydrogen (frames a and b) and hydroxylamine (frames c and d) concentration profiles are shown for one time for two simulations. In frames a and c the reaction rates are relatively slow, compared with the mass transfer, but in frames b and d the reaction is relatively fast. From Radl et al.



Approximate

$$M_0 = \int_0^\infty f \, dn$$

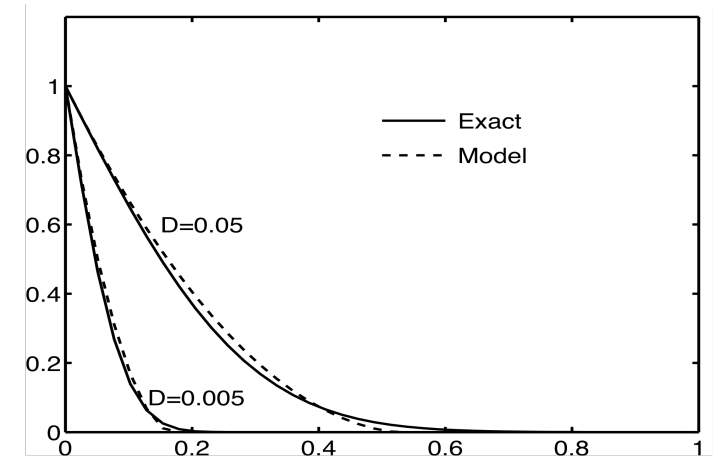
$$M_1 = \int_0^\infty n f \, dn$$

$$\frac{dM_0}{dt} = -2\sigma M_0 + 4D \left. \frac{\partial f}{\partial n} \right|_0$$

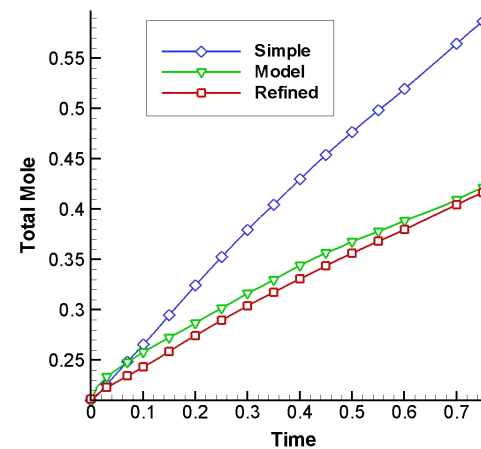
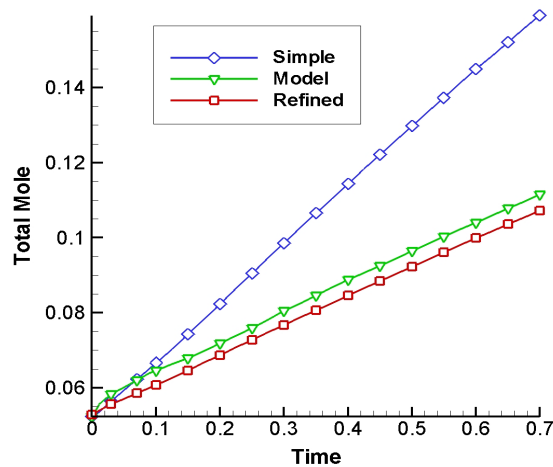
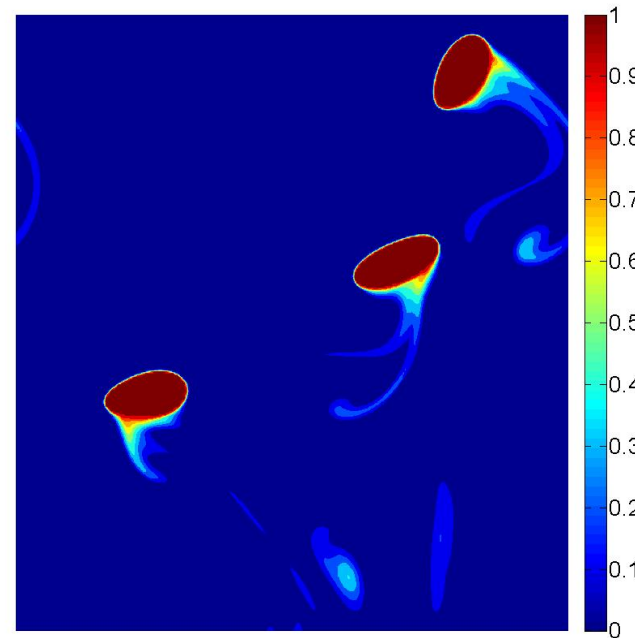
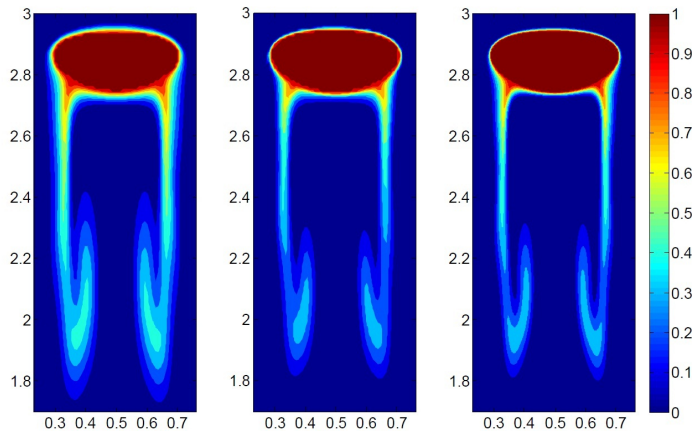
$$\frac{dM_1}{dt} = -3\sigma M_1 + 4Df_0$$

In the mass boundary layer

$$\frac{\partial f}{\partial t} = \sigma n \frac{\partial f}{\partial n} + D \frac{\partial^2 f}{\partial n^2}$$

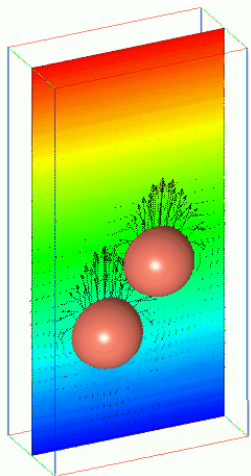


Low resolution; Fully resolved;
Low resolution with model

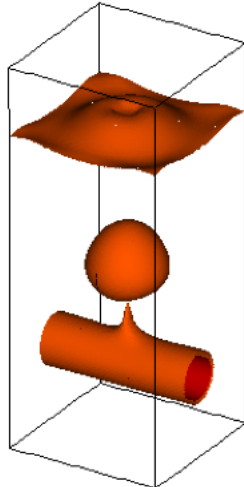


DNS of Multiphase Flows And Many More!

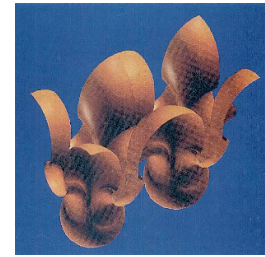
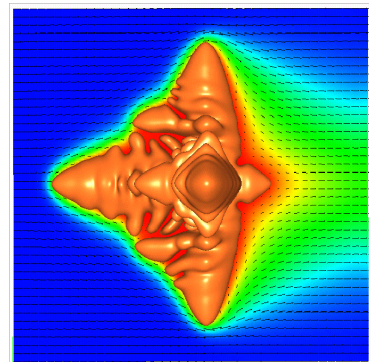
Thermo-capillary migration



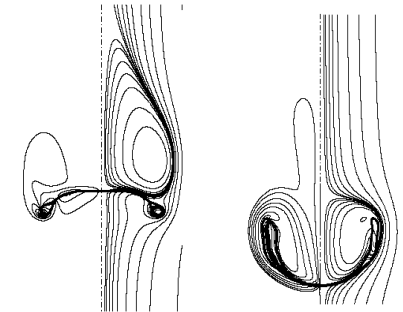
Film boiling from a hot cylinder



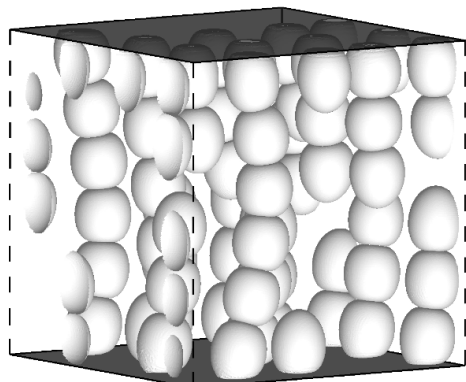
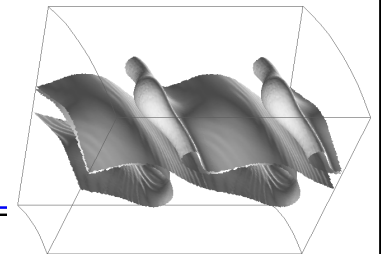
Effect of flow on dendritic solidification



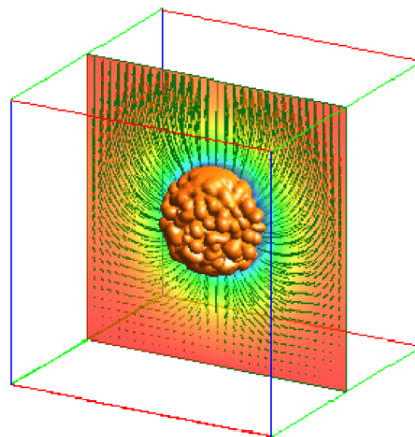
Rayleigh-Taylor



Drop breakup

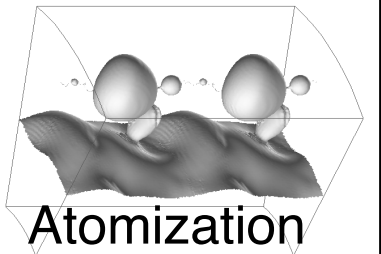
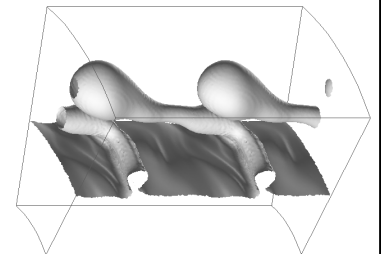
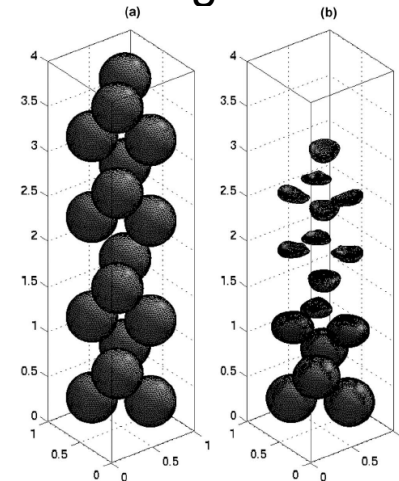


Fibrations due to electric fields



Explosive Boiling

Cavitating bubbles



Atomization



DNS of Multiphase Flows Summary

The front tracking method described here has the right combination of simplicity and accuracy to allow simulation of fairly complex multiphase flow problems.

The control over topology changes provides the user with the ability to either include or exclude such changes.

Generally, explicit tracking provides more accurate results for the same resolution than marker function methods, but at the cost of slightly more complexity.

The presence of separate computational elements to track the front allows for many extensions and improvements



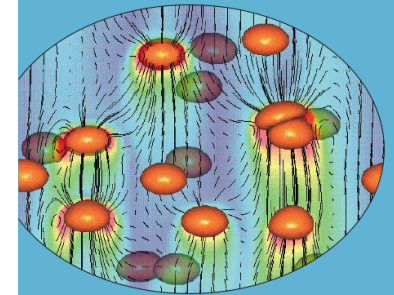
DNS of Multiphase Flows What Now?

We now have the ability to conduct DNS of disperse multiphase flows for a fairly large range of situations. These simulations have been shown to yield insight of the same type obtained from DNS of single phase turbulent flows

Modeling of multiphase flows is far behind single phase flows and the development of more advanced models that can incorporate the new insight and data is perhaps the most urgent task in computational studies of multiphase flows

Numerical challenges still remain, but those are of critical importance primarily for flows that are more complex than those discussed here (churn-turbulent, phase change, etc.)

One of the biggest obstacle for more rapid increase in the use of DNS is the high “entry barrier” for new investigators. Many “things” to learn!



Computational Methods
for Multiphase Flow

Edited by Andrea Prosperetti and Grétar Tryggvason

CAMBRIDGE

Direct Numerical Simulations
of Gas-Liquid Multiphase Flows

Grétar Tryggvason,
Ruben Scardovelli and Stéphane Zaleski



CAMBRIDGE